

# LRFTubes documentation - v1.1

Dr.ir. J.A. de Jong

May 25, 2021



ASCEE  
Maximastraat 1  
7442 NW Nijverdal  
The Netherlands  
T: +31 6 18971622  
E: info@ascee.nl

---

Internal document ID:	628318
Document status:	Draft
Document revision:	1
Revision history:	2018-02-21: rev. 1

---

Copyright (©) 2021 ASCEE. All rights reserved.

# Contents

<b>Contents</b>	<b>2</b>
<b>List of symbols</b>	<b>5</b>
<b>1 Overview of LRFTubes</b>	<b>7</b>
1.1 Introduction	7
1.2 License and disclaimer	7
1.3 Features	7
1.3.1 Limitations and future features	8
1.3.1.1 Ducts with (turbulent) flow	8
1.3.1.2 Porous acoustic absorbers	8
1.4 Overview of this documentation	8
<b>2 Material properties</b>	<b>9</b>
2.1 Air	9
2.2 Exhaust gas	9
2.2.1 Composition	9
2.2.2 Ideal gas mixtures	9
2.2.3 Transport properties	10
2.2.3.1 Dynamic viscosity of pure gases	10
2.2.3.2 Dynamic viscosity of a gas mixture	10
2.2.3.3 Thermal conductivity of a gas mixture	10
2.2.4 Combustion	11
2.2.5 Specific heat ratio	12
2.3 Sound absorbing solid materials	12
<b>3 The transfer matrix method</b>	<b>13</b>
3.1 Introduction	13
3.2 Example transfer matrix of an acoustic duct	13
3.3 Setting up the system of equations	14
3.4 Input impedance, output impedance	15
<b>4 Provided acoustic models</b>	<b>17</b>
4.1 Introduction	17
4.2 Prismatic duct	17
4.2.1 Other cross-sectional geometries	18
4.2.1.1 Rectangular duct	18
4.2.1.2 Annular ring	18
4.2.2 Transfer matrix	19
4.3 Duct with varying cross-sectional area	20
4.3.1 Exponential duct (horn)	20
4.3.2 Conical ducts	20
4.4 Prismatic lined circular duct	21
4.5 Prismatic duct with flow	21

4.6	Cremers impedance	22
4.6.1	Locally reacting lining with back-volume	22
4.7	Cavity silencer	22
4.8	Compliance volume	23
4.9	Membrane	23
4.10	Hole	23
4.11	End corrections and discontinuities	24
4.12	Hard wall	24
4.13	Spherical wave propagation models	26
4.14	Boundary conditions	26
4.14.1	Radiation impedance of a baffled piston	26
<b>5</b>	<b>Speaker</b>	<b>27</b>
5.1	As an active element, with voltage control	27
5.2	As antireciprocal segment	28
<b>6</b>	<b>Optimized reactive silencers</b>	<b>29</b>
6.1	Parallel Helmholtz resonator transfer function and transmission loss	29
6.1.1	Transmission loss	30
6.1.2	Insertion loss	31
6.1.3	Insertion loss for a Helmholtz side branch resonator	32
6.1.3.1	High output impedance limit ( $Z_s \gg Z_{\text{rad}}$ ), volume flow source	32
6.1.3.2	Low output impedance limit ( $Z_s \ll Z_{\text{rad}}$ ), pressure source	32
6.1.3.3	Special case: barrier in an infinite space ( $Z_s = Z_{\text{rad}}$ )	32
6.1.4	Multiple Helmholtz resonators at a single inlet	32
6.2	Transmission of the duct	32
<b>7</b>	<b>(Micro)-perforated plate design</b>	<b>33</b>
7.1	Tuning the hole diameter for large holes and the negligible hole-hole interaction	34
7.1.1	COMSOL boundary condition to useful	34
7.1.2	Porosity estimator constraint	34
7.2	Large hole (boundary layer) limit	35
7.2.1	Lots of holes	35
7.2.2	Some holes	36
7.3	Small hole limit	36
7.4	Geometry of hole patterns	36
7.5	Addition of acoustic hole resistance in an otherwise inviscid simulation	36
7.6	Over-all transmission matrix	37
<b>8</b>	<b>Miscellaneous models for acoustic components</b>	<b>38</b>
8.1	Acoustic impedance of small orifices	38
8.1.1	Rectangular orifice	38
8.1.2	Slit orifice	38
<b>9</b>	<b>Lookup model</b>	<b>39</b>
<b>10</b>	<b>IEC Coupler impedances</b>	<b>40</b>
<b>11</b>	<b>Kampinga's SLNS model in our notation</b>	<b>41</b>
11.1	Model	41
	<b>Bibliography</b>	<b>42</b>
<b>A</b>	<b>Thermal relaxation in thick tubes</b>	<b>43</b>
A.1	Thermal relaxation effect in thick tubes	43

<b>B Derivation of Karal's discontinuity factor</b>	<b>45</b>
B.1 Boundary conditions . . . . .	46

# List of symbols

## Roman symbols

$\ell$	Characteristic length scale of a fluid space	[m]
$\mathbf{n}$	Normal vector pointing from the solid into the fluid	[-]
$\mathbf{r}$	Transverse position vector	[-]
$\mathbf{u}$	Velocity vector	[m·s <sup>-1</sup> ]
$\mathbf{x}$	Position vector	[m]
$a$	Tube radius	[m]
$c$	Speed of sound	[m·s <sup>-1</sup> ]
$C_c$	Acoustic capacitance of a compliance volume	[m <sup>3</sup> ·Pa <sup>-1</sup> ]
$c_p$	Specific heat at constant pressure	[J·kg <sup>-1</sup> ·K <sup>-1</sup> ]
$c_s$	Specific heat of the solid	[J·kg <sup>-1</sup> ·K <sup>-1</sup> ]
$c_v$	Specific heat at constant density	[J·kg <sup>-1</sup> ·K <sup>-1</sup> ]
$D$	Diameter	[m]
$e$	Thermal effusivity	[J·m <sup>-2</sup> ·K <sup>-1</sup> ·s <sup>-½</sup> ]
$f$	Frequency	[Hz]
$f_\kappa$	Thermal Rott function	[-]
$f_\nu$	Viscous Rott function	[-]
$i$	Imaginary unit	[-]
$j$	Index, subscript placeholder	[-]
$J_\alpha$	Bessel function of the first kind and order $\alpha$	
$k$	Wave number	[rad·m <sup>-1</sup> ]
$L$	Length	[m]
$M_A$	Acoustic mass	[kg·m <sup>-4</sup> ]
$N$	Number of	[-]
$N$	Number	[-]
$p$	Pressure, acoustic pressure	[Pa]
$r$	Radial position in cylindrical coordinates	[m]
$r_h$	Hydraulic radius	[m]
$S$	Cross-sectional area, surface area	[m <sup>2</sup> ]
$T$	Temperature	[K]
$t$	Time	[s]
$U$	Volume flow	[m <sup>3</sup> ·s <sup>-1</sup> ]
$u$	Velocity in wave propagation direction	[m·s <sup>-1</sup> ]
$V$	Volume	[m <sup>3</sup> ]

$Z$	Volume flow impedance . . . . .	$[\text{Pa}\cdot\text{s}\cdot\text{m}^{-3}]$
$z$	Specific acoustic impedance . . . . .	$[\text{Pa}\cdot\text{s}\cdot\text{m}^{-1}]$

**Greek symbols**

$\alpha$	Ratio of tube radii . . . . .	$[-]$
$\chi$	Karal's discontinuity factor . . . . .	$[-]$
$\delta_\kappa$	Thermal penetration depth . . . . .	$[\text{m}]$
$\delta_\nu$	Viscous penetration depth . . . . .	$[\text{m}]$
$\epsilon_s$	Ideal stack correction factor . . . . .	$[-]$
$\Gamma$	Viscothermal wave number for a prismatic duct . . . . .	$[\text{rad}\cdot\text{m}^{-1}]$
$\gamma$	Ratio of specific heats . . . . .	$[-]$
$\lambda$	Wavelength . . . . .	$[\text{m}]$
$\Pi$	Wetted perimeter (contact length between solid and fluid) . . . . .	$[\text{m}]$
$\pi$	Ratio of the circumference to the diameter of a circle . . . . .	$[-]$

**Miscellaneous symbols and operators**

$\bullet$	Placeholder for an operand . . . . .	
$\Im$	Imaginary part . . . . .	
$\ \bullet\ $	Euclidian norm . . . . .	
$\nabla$	Gradient . . . . .	$[\text{m}^{-1}]$
$\nabla^2$	Laplacian . . . . .	$[\text{m}^{-2}]$
$\partial$	Infinitesimal . . . . .	
$\Re$	Real part . . . . .	
$\sim$	Same order of magnitude . . . . .	
$d$	Infinitesimal . . . . .	

**Abbreviations and acronyms**

Eq(s).	Equation(s)
LRF	Low Reduced Frequency
Sec(s).	Section(s)

**Sub- and superscripts**

$f$	Fluid
$i$	Inner
$L$	Left side
$o$	Outer
$R$	Right side
$s$	Solid
$s$	Squeeze
$t$	Tube
$w$	Wall
$0$	Evaluated at the reference condition
wall	At the wall

# Chapter 1

## Overview of LRFTubes

### 1.1 Introduction

Welcome to the documentation of LRFTubes. LRFTubes is a numerical code to solve one-dimensional acoustic duct systems using the transfer matrix method. Segments can be connected to generate simple one-dimensional acoustic systems to model acoustic propagation problems in ducts in the frequency domain. Viscothermal dissipation mechanisms are taken into account such that the damping effects can be modeled accurately, below the cut-on frequency of the duct. For more information regarding the models and the theory behind the models, the reader is referred to the work of [4], [5] and [15].

This documentation serves as a reference for the implemented models. For examples on how to use the code, please take a look at the example models as worked out in the IPython Notebooks. For installation instructions, please refer to the [README](#) in the main repository.

This document is very brief on the theory and it is assumed that the reader has some knowledge on the basics of acoustics in general and viscothermal acoustics as well. If you are not falling in this category, I would please refer you first to the book of Swift [13]. A more detailed introduction to the notation used in this documentation can be found in the PhD thesis of de Jong [3].

Besides that, if you find the work interesting, but you are not sure how to apply it, please contact ASCEE for more information.

### 1.2 License and disclaimer

Redistribution and use in source and binary forms are permitted provided that the above copyright notice and this paragraph are duplicated in all such forms and that any documentation, advertising materials, and other materials related to such distribution and use acknowledge that the software was developed by the ASCEE. The name of the ASCEE may not be used to endorse or promote products derived from this software without specific prior written permission.

THIS SOFTWARE IS PROVIDED “AS IS” AND WITHOUT ANY EXPRESS OR IMPLIED WARRANTIES, INCLUDING, WITHOUT LIMITATION, THE IMPLIED WARRANTIES OF MERCHANTABILITY AND FITNESS FOR A PARTICULAR PURPOSE.

### 1.3 Features

Currently the LRFTubes code provides acoustic models for the following physical entities:

- Prismatic ducts with circular cross section,
- Prismatic ducts with triangular cross section,
- Prismatic ducts with parallel plate cross section,
- Prismatic ducts with square cross section,

- Acoustic compliance volumes
- Discontinuity correction
- End correction for a baffled piston
- Lumped series impedance

These segments can be connected to form one-dimensional acoustic systems to model wave propagation below the cut-on frequency of higher order modes. For a circular cross section, the cut-on frequency is [4]:

$$f_c \approx \frac{c_0}{3.4r}, \quad (1.1)$$

where  $r$  is the tube radius and  $c_0$  is the speed of sound. Above the cut-on frequency, besides evanescent waves, there are also propagating waves with a non-constant pressure distribution along the cross section of the duct.

### 1.3.1 Limitations and future features

The current version of has some limitations that will be resolved in a future release. These are:

#### 1.3.1.1 Ducts with (turbulent) flow

For thermoacoustic and HVAC (Heating, ventilation and Air Conditioning) duct modeling it is imperative that mean flows can be taken into account. An acoustic wave superimposed on a mean flow results in asymmetric wave propagation. More specifically, the phase velocity is higher in the direction of the mean flow, and slower in the opposite direction. In a future release, we will provide models for ducts including a mean flow.

#### 1.3.1.2 Porous acoustic absorbers

To model absorption of sound, a one-dimensional porous material model should be implemented. This work has been postponed to a later stage.

## 1.4 Overview of this documentation

The next chapter of this documentation will describe the basic framework of the LRFTubes code: the transfer matrix method. After that, in Chapter 4, an overview of the provided acoustic models is given, with which acoustic networks can be built. For each of the segments, the resulting transfer matrix model is derived.

## Chapter 2

# Material properties

### 2.1 Air

Nonlinearity parameter:

### 2.2 Exhaust gas

#### 2.2.1 Composition

Definitions:

- $\omega_i$  mass fraction of species  $i$
- $x_i$  molar / volume fraction of species  $i$  (assuming ideal gas behavior)
- $\bar{M}$  average molar mass of (exhaust gas) mixture
- $M_i$  molar mass of species  $i$

The following equations hold in a mixture:

$$\sum_i \omega_i = 1 \quad (2.1)$$

$$\sum_i x_i = 1 \quad (2.2)$$

$$\bar{M} = \sum_i x_i M_i \quad (2.3)$$

We can convert mass fractions to mole fractions with the following rule:

$$\omega_i = x_i \frac{M_i}{\bar{M}} \iff x_i = \omega_i \frac{\bar{M}}{M_i} \quad (2.4)$$

Henceforth, what is often used, is to compute the average molar mass given only the mass fractions:

$$\bar{M} = \frac{1}{\sum_i \frac{\omega_i}{M_i}} \quad (2.5)$$

#### 2.2.2 Ideal gas mixtures

For an ideal gas, the components of a gas mixture can be represented by their “partial pressure”, which is the total pressure times the volume fraction of the component in the mixture. For an ideal gas, the volume fraction equals to mole fraction. Hence:

$$\frac{V_i}{V} \stackrel{\text{ideal gas}}{=} x_i = \frac{p_i}{R_u T} \quad (2.6)$$

The mass fraction can be computed from the mole fraction.

Substance	$M$	$T_c$	$G$	$C_r$
Carbon dioxide	$44.01 \cdot 10^{-3}$ kg/mol	304 K	44.6	0.766
Oxygen	$32.00 \cdot 10^{-3}$ kg/mol	154 K	32.8	0.712
Nitrogen	$28.02 \cdot 10^{-3}$ kg/mol	126 K	24.6	0.881
Water vapor	$18.02 \cdot 10^{-3}$ kg/mol	647 K	52.2	1.018

**Table 2.1** – Critical values and constants of common diatomic gases

## 2.2.3 Transport properties

### 2.2.3.1 Dynamic viscosity of pure gases

Here we assume the dynamic viscosity of a pure substance can be modeled using Sutherland's equation:

$$\mu = \mu_c \left( \frac{T_0 + C}{T + C} \right) \left( \frac{T}{T_0} \right)^{3/2}, \quad (2.7)$$

where the subscript  $c$  denotes the value at its "critical point". In convenient form we solve:

$$\mu = \mu_c \mu_r, \quad (2.8)$$

where  $\mu_c$  is the critical viscosity and  $\mu_r$  is the "reduced viscosity defined as  $\mu/\mu_c$ ". For  $\mu_c$  we have the reduced form of Sutherland's equation:

$$\mu_c = \frac{1 + C_r}{T_r + C_r} T_r^{3/2} \quad (2.9)$$

The value for  $\mu_c$  can be calculated as:

$$\mu_c = 3.5 \cdot 10^{-6} G \quad (2.10)$$

Values for  $T_r$ ,  $C_r$  and  $G$  are listed in Table 2.1 [8].

### 2.2.3.2 Dynamic viscosity of a gas mixture

The dynamic viscosity of a gas mixture can be derived from the dynamic viscosities of pure gases as [1, p. 27]:

$$\mu_{\text{mix}} = \sum_{\alpha=0}^{N-1} \frac{x_{\alpha} \mu_{\alpha}}{\sum_{\beta=0}^{N-1} \Phi_{\alpha\beta} x_{\beta}}, \quad (2.11)$$

where  $\mu_{\alpha}$  is the dynamic viscosity of pure chemical species  $\alpha$  and  $x_{\alpha}$  denotes its mole fraction in the mixture.  $\Phi_{\alpha\beta}$  is defined as:

$$\Phi_{\alpha\beta} = \frac{1}{\sqrt{8}} \left( 1 + \frac{M_{\alpha}}{M_{\beta}} \right)^{-1/2} \left[ 1 + \left( \frac{\mu_{\alpha}}{\mu_{\beta}} \right)^{1/2} \left( \frac{M_{\beta}}{M_{\alpha}} \right)^{1/4} \right]^2, \quad (2.12)$$

where  $M_{\alpha}$  is the molar mass of species  $\alpha$ . The denominator of Eq. 2.11 can efficiently be solved by noting that  $d_{\alpha} = \sum_{\beta=0}^{N-1} \Phi_{\alpha\beta} x_{\beta}$  is a matrix-vector product, which can be written as  $\mathbf{d} = \Phi \cdot \mathbf{x}$ .

### 2.2.3.3 Thermal conductivity of a gas mixture

The thermal conductivity of a gas mixture can be derived from the thermal conductivities of pure gases as [1, p. 276]:

$$k_{\text{mix}} = \sum_{\alpha=0}^{N-1} \frac{x_{\alpha} k_{\alpha}}{\sum_{\beta=0}^{N-1} \Phi_{\alpha\beta} x_{\beta}} \quad (2.13)$$

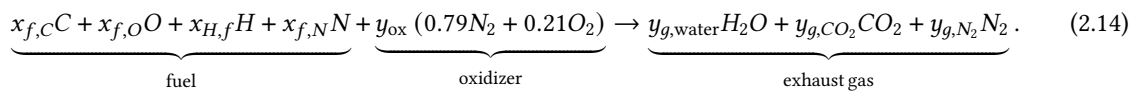
where  $k_{\alpha}$  is the thermal conductivity of pure chemical species  $\alpha$  and  $x_{\alpha}$  denotes its mole fraction in the mixture and  $\Phi_{\alpha\beta}$  is identical to that appearing in the viscosity equation, see 2.12.

Mass fraction	Wood <sup>1</sup>	Dutch Natural gas
Carbon	50 %	
Oxygen	42 %	0 %
Hydrogen	6 %	
Nitrogen	0 %	

**Table 2.2** – Mixture mass composition of fuels

## 2.2.4 Combustion

To compute the gas constant, first the mixture components of the exhaust gas need to be computed. We assume that the oxidizer is air with 79% vol of nitrogen (molecules) and 21% oxygen molecules. The tiny part of argon and other components is ignored. Then, the gross formula for combustion is:



Above reaction formula can be read as: “take  $x_{f,C}$  moles of carbon in the fuel, add  $y_{\text{ox}}$  moles of air, and it should result in  $y_{g,CO_2}$  moles of  $CO_2$ ” And so on for the other elements. The mole fractions in the fuel composition can be derived from its mass fractions, upon utilizing Eqs. 2.4 and 2.5. From Eq. 2.14, the following system of equations can be created:

$$\begin{pmatrix} x_{f,C} \\ x_{f,O} \\ x_{f,H} \\ x_{f,N} \end{pmatrix} + \begin{bmatrix} 0 & 0 & -1 & 0 \\ 2 \times 0.21 & -1 & -2 & 0 \\ 0 & -2 & 0 & 0 \\ 2 \times 0.79 & 0 & 0 & -2 \end{bmatrix} \begin{pmatrix} y_{\text{ox}} \\ y_{g,\text{water}} \\ y_{g,CO_2} \\ y_{g,N_2} \end{pmatrix} = \begin{pmatrix} 0 \\ 0 \\ 0 \\ 0 \end{pmatrix} \quad (2.15)$$

Solving this results in:

$$y_{g,CO_2} = x_{f,C} \quad (2.16)$$

$$y_{g,\text{water}} = \frac{1}{2}x_{f,H} \quad (2.17)$$

$$y_{\text{ox}} = \frac{\frac{1}{2}x_{f,H} + 2x_{f,C} - x_{f,O}}{2 \times 0.21} \quad (2.18)$$

$$y_{g,N_2} = 0.79y_{\text{ox}} + \frac{1}{2}x_{f,N} \quad (2.19)$$

Note that the mole fractions are *unnormalized* (that is why we use symbol  $y$ , not  $x$ ): they denote the number of moles required to burn 1 mole of fuel. To compute the mole fractions in the exhaust gas,

$$x_{g,\text{water}} = \frac{y_1}{y_1 + y_2 + y_3} \quad (2.20)$$

Table 2.2 gives an overview of the composition of typical combustion fuels. Once the molar fractions of the exhaust gas are known, the average molar mass can be computed using Eq. 2.3. Then, the specific gas constant can be computed according to:

$$R_s = \frac{R_u}{M}, \quad (2.21)$$

where  $R_u$  is the universal gas constant.

<sup>1</sup>[https://www.engineeringtoolbox.com/co2-emission-fuels-d\\_1085.html](https://www.engineeringtoolbox.com/co2-emission-fuels-d_1085.html)

Name	Basotect TG <sup>2</sup>
Description	Melamine resin foam (fire retardant)
Density [kg·m <sup>-3</sup> ]	<sup>3</sup>
Flow resistivity [Pa·s·m <sup>-1</sup> ]	8.5·10 <sup>3</sup> , source: [7], Table 2 average value.

**Table 2.3** – Resistivity values are given for room temperature

### 2.2.5 Specific heat ratio

The specific heat is build-up according to mass percentages of the flue gas. Carbon dioxide has a  $c_p$  of 840 J/kg/K, water vapor of 1930:

$$\bar{c}_p = \sum_i \omega_i c_{p,i}. \quad (2.22)$$

### 2.3 Sound absorbing solid materials

High porosity soft materials can be modeled adequately with the Delaney-Bazley-Miki model. The model has a single input, namely the static flow resistivity. Table

Conversion

<sup>2</sup>A.k.a.Flamex Basic (akoestiekwinkel.nl)

<sup>3</sup>[https://www.forman.co.nz/media/emizen\\_banner/b/a/basf\\_basotect\\_datasheet.pdf](https://www.forman.co.nz/media/emizen_banner/b/a/basf_basotect_datasheet.pdf)

## Chapter 3

# The transfer matrix method

### 3.1 Introduction

Each part of an acoustic system in LRFTubes is modeled using a so-called transfer matrix. A transfer matrix maps the state quantities on one side of the segment (node) to the other side of the segment (node).

For one-dimensional wave propagation, analytical solutions for the velocity, temperature and density field in the transverse direction can be found. The state variables in frequency domain satisfy a system of first order ordinary differential equations. Once the solution is known on one end of a segment, the solution on the other end can be deduced. The transfer matrix couples the state variables  $\phi$  on one end of a segment to the other end, in frequency domain:

$$\phi_R(\omega) = T(\omega)\phi_L(\omega) + \mathbf{s}(\omega), \quad (3.1)$$

where  $L$  and  $R$  denote the left and right side, respectively,  $T$  denotes the transfer matrix and  $\mathbf{s}$  is a source term. In the code and in this documentation  $e^{+i\omega t}$  convention is used. A common choice of state variables is such that their product has the unit of power. For all systems in this code, the state variables satisfy this property. For example in an acoustic segment, the power is the product of acoustic pressure  $p(\omega)$  and volume flow  $U(\omega)$ . For complex phasors and, the acoustic power flow can then be computed as:

$$E = \frac{1}{2} \Re [pU^*], \quad (3.2)$$

where  $\Re[\bullet]$  denotes the real part of  $\bullet$ , and  $*$  denotes the complex conjugation.

### 3.2 Example transfer matrix of an acoustic duct

This section will provide the derivation of the transfer matrix of a simple acoustic duct. Starting with the isentropic acoustic continuity and momentum equation :

$$\frac{1}{c_0^2} \frac{\partial \hat{p}}{\partial \hat{t}} + \rho_0 \nabla \cdot \hat{\mathbf{u}} = 0, \quad (3.3)$$

$$\rho_0 \frac{\partial \hat{\mathbf{u}}}{\partial \hat{t}} + \nabla \hat{p} = 0. \quad (3.4)$$

The next step is to transform these equations to frequency domain and assuming only wave propagation in the  $x$ -direction, integrating over the cross section we find:

$$\frac{i\omega}{c_0^2} p + \frac{\rho_0}{S_f} \frac{dU}{dx} = 0, \quad (3.5)$$

$$\rho_0 i\omega U + S_f \frac{dp}{dx} = 0, \quad (3.6)$$

where  $U$  denotes the acoustic volume flow in  $\text{m}^3 \cdot \text{s}^{-1}$ . Eqs. (3.5-3.6) is a coupled set of ordinary differential equations, which can be solved for the acoustic pressure to find

$$p(x) = A \exp(-ikx) + B \exp(ikx), \quad (3.7)$$

where  $A$  and  $B$  are constants, to be determined from the boundary conditions. Setting  $p = p_L$ , and  $U = U_L$  at  $x = 0$ , we can solve for the acoustic pressure, upon using Eq. 3.6 as:

$$p(x) = p_L \cos(kx) - iZ_0 \sin(kx) U_L, \quad (3.8)$$

and for the acoustic volume flow we find:

$$U(x) = U_L \cos(kx) - \frac{i}{Z_0} \sin(kx) p_L. \quad (3.9)$$

Now, we have all ingredients to derive the transfer matrix of an acoustic duct. Setting  $p(x = L) = p_R$ , and  $U(x = L) = U_R$ , we find the following two-port coupling between the pressure and the velocity from the left side of the duct to the right side of the duct:

$$\begin{Bmatrix} p_R \\ U_R \end{Bmatrix} = \begin{bmatrix} \cos(kL) & -iZ_0 \sin(kL) \\ -iZ_0^{-1} \sin(kL) & \cos(kL) \end{bmatrix} \begin{Bmatrix} p_L \\ U_L \end{Bmatrix}. \quad (3.10)$$

### 3.3 Setting up the system of equations

LRFTubes has been set up to solve systems of acoustic segments such as this prismatic duct. The advantage of the transfer matrix method is the ease with which mixed (impedance/pressure/velocity) boundary conditions can be implemented.

In this section, the assembly of the global system of equations is explained. The state variables of each segment are stacked in a column vector  $\phi_{\text{sys}}$ , which has the size of  $4N_{\text{segs}}$ , where  $N_{\text{segs}}$  denotes the number of segments in the system. The coupling equations between the nodes of each segment, are the transfer matrices. Since the transfer matrices are  $2 \times 2$ , this fills only half of the required amount of equations. The other half is filled with boundary conditions. Each segments transfer matrix can be regarded as the element matrix, which all have a form like:

$$\phi_R = T \cdot \phi_L + s, \quad (3.11)$$

where  $\phi_L, \phi_R$  are the state vectors on the left and right sides of the segment, respectively,  $T$  is the transfer matrix, and  $s$  is a source term.

There are two kind of boundary conditions, called external and internal boundary conditions. External boundary conditions apply where a prescribed condition is given, such as a prescribed pressure, voltage, volume flow, current or acoustic/electric impedance. Internal boundary conditions are used to couple different segments at a connection point, which is recognized by a shared node number. At a connection point, the effort variable is shared, which means that the pressure at the node is equal for each connected segment sharing the node. The flow variable is conserved, so the sum of the volume flow out of all segments connected at the node is 0.

#### Example: two ducts

This procedure of creating a system matrix is explained by an example where only two ducts are coupled. A schematic of the situation is depicted in Figure 3.1. For the example situation, at the left node of segment (1), an impedance boundary  $Z_L$  is prescribed. The right node of segment (1) is connected to the left node of segment (2), and at the right side of segment (2), a volume flow boundary condition is prescribed of  $U_R$ . The corresponding system of equations for this case is

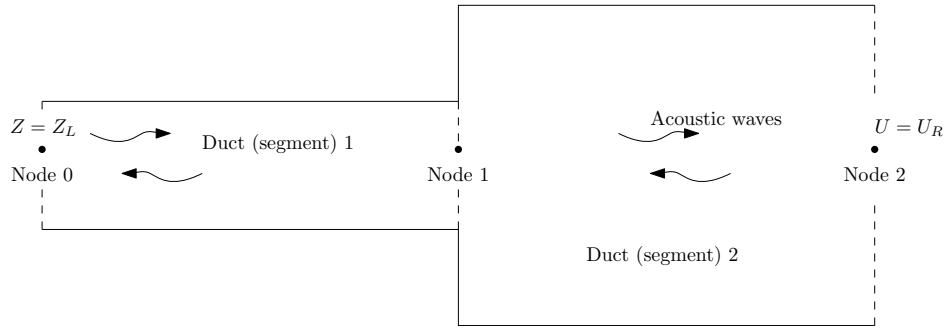


Figure 3.1 – Example of two simple duct segments connected together.

$$\begin{bmatrix}
 \mathbf{T}_1 & -\mathbf{I} & \mathbf{0} & \mathbf{0} \\
 \mathbf{0} & \mathbf{0} & \mathbf{T}_2 & -\mathbf{I} \\
 \mathbf{0} & \begin{bmatrix} 1 & 0 \\ 0 & 1 \end{bmatrix} & \begin{bmatrix} -1 & 0 \\ 0 & -1 \end{bmatrix} & \mathbf{0} \\
 \begin{bmatrix} 1 & Z_L \\ 0 & 0 \end{bmatrix} & \mathbf{0} & \mathbf{0} & \begin{bmatrix} 0 & 0 \\ 0 & 1 \end{bmatrix}
 \end{bmatrix}
 \begin{pmatrix}
 p_{1L} \\
 U_{1L} \\
 p_{1R} \\
 U_{1R} \\
 p_{2L} \\
 U_{2L} \\
 p_{2R} \\
 U_{2R}
 \end{pmatrix}
 =
 \begin{pmatrix}
 0 \\
 0 \\
 0 \\
 0 \\
 0 \\
 0 \\
 0 \\
 U_R
 \end{pmatrix}, \quad (3.12)$$

In this system matrix,  $\mathbf{0}$  denotes a  $2 \times 2$  sub matrix of zeros and  $\mathbf{I}$  denotes a  $2 \times 2$  identity sub matrix.  $\mathbf{T}_i$  is the transfer matrix of the  $i$ -th segment. The solution can be obtained by Gaussian elimination, for which in LRFTubes the `numpy.linalg.solve()` solver is used. Once the solution on the nodes is known, the solution in each segment can be computed as a post processing step. LRFTubes provides some post processing routines to aid in visualization of the acoustic field inside a non-lumped segment, such as an acoustic duct.

### 3.4 Input impedance, output impedance

The acoustic input impedance  $Z_{in} \equiv p_L/U_L$  on the left side of a segment is defined as the impedance a connecting segment “feels” for a certain boundary condition on the right side.<sup>1</sup> There are two special load cases for the segment, either on the right side, the circuit is open, resulting in  $U_R = 0$ , or the circuit is shorted, which results in  $p_R = 0$ . For the open circuit, the input impedance can be computed from the transfer matrix as:

$$Z_{in,open} = -\frac{T_{22}}{T_{21}} \quad (3.13)$$

$$Z_{in,short} = -\frac{T_{12}}{T_{11}} \quad (3.14)$$

For a passive component (and passive load on the right side), the real part of the input impedance should be positive:

$$\Re [Z_{in}] \geq 0. \quad (3.15)$$

The acoustic output impedance  $Z_{out} \equiv p_R/U_R$  on the right side of a segment is defined as the impedance a

<sup>1</sup>Note that the definitions of open and closed below are relating to electrical circuits, not open or closed in the acoustical sense. I.e. an open impedance corresponds to a hard acoustic wall (which is acoustically closed).

connecting segment “feels” for a certain boundary condition on the left side.

$$Z_{\text{out,open}} = \frac{T_{11}}{T_{21}} \quad (3.16)$$

$$Z_{\text{out,short}} = \frac{T_{12}}{T_{22}} \quad (3.17)$$

For passive segments, the real part of the output impedance should be *negative*:

$$\Re [Z_{\text{out}}] \leq 0. \quad (3.18)$$

## Chapter 4

# Provided acoustic models

### 4.1 Introduction

This chapter provides a concise overview of the provided acoustic models implemented in LRFTubes.

### 4.2 Prismatic duct

A prismatic duct is used to model one-dimensional acoustic wave propagation. The prismatic duct is implemented in LRFTubes in the PRSDuct class. Figure 4.1 shows this segment schematically. In the thermal boundary layer, heat and momentum diffuse to the wall. The thermal boundary layer can be a small layer w.r.t. to the transverse characteristic length scale of the tube, or can fully occupy the tube. In the latter case, the solution converges to the classic laminar Poiseuille flow solution. The basic assumptions behind this model are

- Prismatic cross sectional area.
- $L \gg r_h$ , (tube is long compared to its transverse length scale).
- Radius is much smaller than the wave length.
- Wave length is much larger than viscous penetration depth.
- End effects and entrance effects are negligible.

For a formal derivation of the model for prismatic cylindrical tubes, the reader is referred to the work of Tijdeman [14] and Nijhof [9]. For a somewhat more pragmatic derivation, we would like to refer to the work of Swift [13, 12] and Rott [11].

$$\frac{dp}{dx} = \frac{\omega \rho_0}{i(1 - f_v) S_f} U, \quad (4.1)$$

$$\frac{dU}{dx} = \frac{k}{iZ_0} \left( 1 + \frac{(\gamma-1)f_k}{1+\epsilon_s} \right) p, \quad (4.2)$$

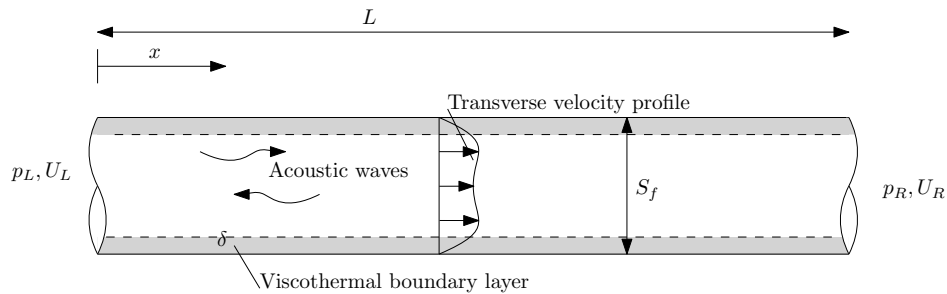


Figure 4.1 – Geometry of the prismatic duct

where  $S_f$  is the cross-sectional area filled with fluid,  $k$  is the inviscid wave number, and  $Z_0$  the inviscid characteristic impedance of a tube ( $Z_0 = z_0/S_f$ ).  $f_v$  and  $f_\kappa$  are the viscous and thermal Rott functions, respectively [11]. They model the viscous and thermal effects with the wall. For circular tubes, the  $f$ 's are defined as [13, p. 88]:

$$f_{j,\text{circ}} = \frac{J_1 \left[ (i-1) \frac{2r_h}{\delta_j} \right]}{(i-1) \frac{r_h}{\delta} J_0 \left[ (i-1) \frac{2r_h}{\delta_j} \right]}, \quad (4.3)$$

where  $\delta_j = \delta_v$  for  $f_{v,\text{circ}}$  and  $\delta_j = \delta_\kappa$  for  $f_{\kappa,\text{circ}}$ .  $J_\alpha$  denotes the cylindrical Bessel function of the first kind and order  $\alpha$ .  $r_h$  is the hydraulic radius, defined as the ratio of the cross sectional area to the “wetted perimeter”:

$$r_h = S_f / \Pi. \quad (4.4)$$

Note that for a circular tube with diameter  $D$ ,  $r_h = D/4$ . The parameter  $\epsilon_s$  in Eq. 4.2 is the ideal solid correction factor, which corrects for solids that have a finite heat capacity. This parameter is dependent on the thermal properties and the geometry of the solid. An example of  $\epsilon_s$  is derived in Section A.1. For the case of an thermally ideal solid,  $\epsilon_s$  can be set to 0.

## 4.2.1 Other cross-sectional geometries

### 4.2.1.1 Rectangular duct

Analytical functions exist for prismatic geometries, such as parallel plates, rectangular holes, and even triangular holes. For parallel plates with sides  $2y_0 \times 2z_0$ , the Rott function reads:

$$f = 1 - \frac{64}{\pi^4} \sum_{n=1}^{\infty} \sum_{m=1}^{\infty} \frac{1}{(2m-1)^2} \frac{1}{(2n-1)^2} \frac{1}{C_{mn}}, \quad (4.5)$$

where

$$C_{mn} = 1 - \frac{i\pi^2 \delta^2}{8y_0^2 z_0^2} \left( (2m-1)^2 z_0^2 + (2n-1)^2 y_0^2 \right). \quad (4.6)$$

The hydraulic radius is related to  $y_0$  and  $z_0$  as:

$$r_h = \frac{y_0 z_0}{y_0 + z_0} \quad (4.7)$$

Defining the aspect ratio as  $\mathcal{R} = z_0/y_0$ , a useful equation is to derive  $y_0$  and  $z_0$  from  $r_h$  and  $\mathcal{R}$ :

$$y_0 = r_h \frac{(1 + \mathcal{R})}{\mathcal{R}} \quad (4.8)$$

$$z_0 = r_h (1 + \mathcal{R}) \quad (4.9)$$

### 4.2.1.2 Annular ring

The differential equation that is required to be solved

$$\frac{i\mu_0}{\omega \rho_0} \nabla_{\perp}^2 h_v + h_v = 0, \quad h_v|_{\text{wall}} = 0 \quad (4.10)$$

For an annular duct the Rott function reads:

$$h_v = \frac{\left( J_0 \left( \frac{r_0(1-i)}{\delta_v} \right) - J_0 \left( \frac{r_1(1-i)}{\delta_v} \right) \right) Y_0 \left( \frac{r(1-i)}{\delta_v} \right) + \left( Y_0 \left( \frac{r_1(1-i)}{\delta_v} \right) - Y_0 \left( \frac{r_0(1-i)}{\delta_v} \right) \right) J_0 \left( \frac{r(1-i)}{\delta_v} \right)}{J_0 \left( \frac{r_0(1-i)}{\delta_v} \right) Y_0 \left( \frac{r_1(1-i)}{\delta_v} \right) - J_0 \left( \frac{r_1(1-i)}{\delta_v} \right) Y_0 \left( \frac{r_0(1-i)}{\delta_v} \right)}$$

Where

$$\alpha_0 = \frac{r_0 (1 - i)}{\delta_i}$$

$$\alpha_1 = \frac{r_1 (1 - i)}{\delta_i}$$

And:

$$C_1 = \frac{Y_0(\alpha_1) - Y_0(\alpha_0)}{J_0(\alpha_0) Y_0(\alpha_1) - J_0(\alpha_1) Y_0(\alpha_0)} \quad (4.11)$$

$$C_2 = \frac{J_0(\alpha_0) - J_0(\alpha_1)}{J_0(\alpha_0) Y_0(\alpha_1) - J_0(\alpha_1) Y_0(\alpha_0)} \quad (4.12)$$

$$f_i = \delta_i (1 + i) \frac{\left\{ H_0^{(1)}(\alpha_0) - H_0^{(1)}(\alpha_1) \right\} \left[ r_0 H_{-1}^{(2)}(\alpha_0) - r_1 H_{-1}^{(2)}(\alpha_1) \right] + \left\{ H_0^{(2)}(\alpha_0) - H_0^{(2)}(\alpha_1) \right\} \left[ r_1 H_{-1}^{(1)}(\alpha_1) - r_0 H_{-1}^{(1)}(\alpha_0) \right]}{(r_1^2 - r_0^2) \left[ H_0^{(1)}(\alpha_0) H_0^{(2)}(\alpha_1) - H_0^{(1)}(\alpha_1) H_0^{(2)}(\alpha_0) \right]} \quad (4.13)$$

#### 4.2.2 Transfer matrix

Upon solving for Eqs. 4.1-4.2, a transfer matrix can be derived which couples the pressure and volume flow on the left side to the right side as:

$$\begin{Bmatrix} p_R \\ U_R \end{Bmatrix} = \begin{bmatrix} \cos(\Gamma L) & -iZ_c \sin(\Gamma L) \\ -iZ_c^{-1} \sin(\Gamma L) & \cos(\Gamma L) \end{bmatrix} \begin{Bmatrix} p_L \\ U_L \end{Bmatrix}, \quad (4.14)$$

where  $Z_c$  is the characteristic impedance of the duct, i.e. the impedance  $p/U$  of a plane (although damped) propagating wave:

$$Z_c = \frac{kZ_0}{(1 - f_v)\Gamma}. \quad (4.15)$$

The parameter  $\Gamma$  in Eqs. 4.14 and 4.15 is the viscothermal wave number, i.e. the wave number corrected for viscothermal losses:

$$\Gamma = \frac{\omega}{c_0} \sqrt{\frac{1 + \frac{(\gamma-1)f_c}{1+\epsilon_s}}{1 - f_v}}. \quad (4.16)$$

Due to the numerical implementation of the Bessel functions in many libraries, the  $f_j$  function for cylindrical ducts (Eq. 4.3) cannot be computed for high  $r_h/\delta$  by computing this ratio  $J_1/J_0$ . The numerical result starts to break down at  $r_h/\delta \sim 100$ . To resolve this problem, the LRFTubes code applies a smooth transition from the Bessel function ratio to the boundary layer limit solution for  $f$ :

$$f_{j,bl} = \frac{(1 - i)\delta_j}{2r_h} \quad (4.17)$$

in the range of  $100 < r_h/\delta \leq 200$ .

Note that in the limit of  $r_h \rightarrow \infty$ , or  $\kappa$  and  $\mu \rightarrow 0$ ,  $\Re[\Gamma] \rightarrow k$  and  $\Re[Z_c] \rightarrow Z_0$  whereas  $\Im[\Gamma]$  and  $\Im[Z_c] \rightarrow 0$ . Hence in these limits the lossless wave equation is resolved from the result. This is not true in the limit of  $\omega \rightarrow \infty$ , as in that limit it can be computed that  $\Re[\Gamma] \rightarrow k$ , while the imaginary part

$$-\Im[\Gamma] \rightarrow \sqrt{\omega} \frac{\sqrt{\frac{1}{8} \frac{\mu}{\rho_0}}}{c_0 r_h} \left[ 1 + \frac{(\gamma - 1)}{\sqrt{\text{Pr}}} \right]. \quad (4.18)$$

In other words the imaginary part of the wave number keeps growing, although with a smaller rate than real part of the wave number. So the higher the frequency, the smaller the viscothermal damping per wavelength, but the higher the viscothermal damping per meter of duct.

Figure 4.2 shows the imaginary part of the wave number as a function of the frequency. As visible, the magnitude of the viscothermal damping grows monotonically with frequency.

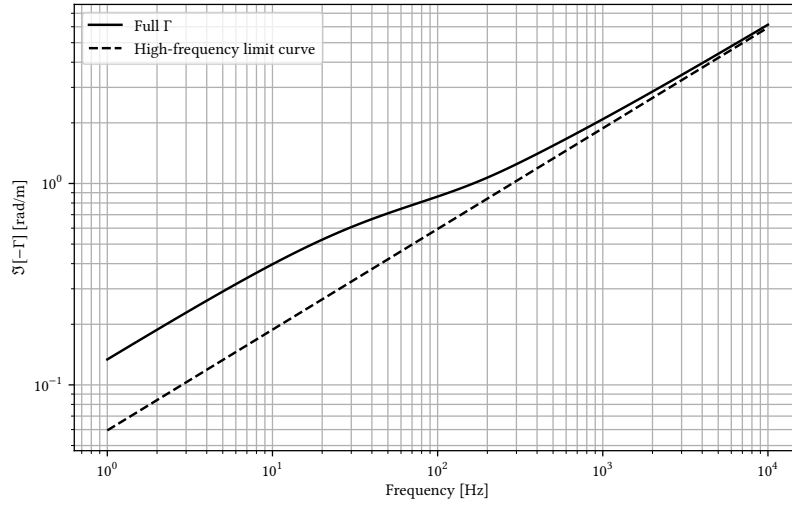


**Figure 4.2** – Logarithmic plot of the negative of imaginary part of the viscothermal wave number ( $-\Im[\Gamma]$ ), for a tube with a diameter of 1 mm. In blue, the full  $f_v$  and  $f_c$  of Eq. 4.16 and 4.3 is used. The orange curve corresponds to Eq. 4.18.

### 4.3 Duct with varying cross-sectional area

For ducts with variation in the cross-sectional area, an approximately valid ordinary differential equation can be derived, which is a viscothermal correction to Webster's horn equation [10, p. 181]:

$$\frac{d^2 p}{dx^2} + \frac{1}{S_f} \frac{dS_f}{dx} \frac{dp}{dx} + \Gamma^2 p = 0 \quad (4.19)$$

#### 4.3.1 Exponential duct (horn)

$$S_f = \exp(\alpha x) \quad (4.20)$$

#### 4.3.2 Conical ducts

For conical ducts, i.e. ducts with quadratic variation in the cross-sectional area (linear variation in the diameter, or cross-sectional length scale),

such that for a conical tube the radius  $r(x)$  varies as:

$$r(x) = r_0 + \eta x, \quad (4.21)$$

where

$$\eta = \frac{x}{L} (r_1 - r_0) \quad (4.22)$$

Filling in for  $S_f = \pi (r_0 + \eta x)^2$  yields

$$\frac{d^2 p}{dx^2} + \frac{2\eta}{r_0 + \eta x} \frac{dp}{dx} + \Gamma^2 p = 0, \quad (4.23)$$

for which the solution is:

$$p = \frac{C_1 \exp(-i\Gamma x) + C_2 \exp(-i\Gamma x)}{r_0 + \eta x} \quad (4.24)$$

$$\mathbf{T}_{\text{cone}} = \begin{bmatrix} \frac{\Gamma r_0 \cos(\Gamma L) + \eta \sin(\Gamma L)}{\Gamma r_1} & -iZ_{c,0} \frac{kr_0 \sin(\Gamma L)}{\Gamma r_1} \\ \frac{iL\eta^2 \cos(\Gamma L)}{\Gamma Z_{c0} r_0^2} - \frac{i}{Z_{c0}} \left( \frac{r_1}{r_0} + \frac{\eta^2}{\Gamma^2 r_0^2} \right) \sin(\Gamma L) & \frac{r_1}{r_0} \cos(\Gamma L) - \frac{\eta \sin(\Gamma L)}{\Gamma r_0} \end{bmatrix}, \quad (4.25)$$

where

$$Z_{c,0} = \frac{\omega \rho_0}{(1 - f_v) S_{f,0} \Gamma_0} \quad (4.26)$$

#### 4.4 Prismatic lined circular duct

The Fourier transformed wave equation in axisymmetric cylindrical coordinates can be written as:

$$\frac{\partial^2 p}{\partial r^2} + \frac{1}{r} \frac{\partial p}{\partial r} + \frac{\partial^2 p}{\partial x^2} + k^2 p = 0, \quad (4.27)$$

Using separation of variables:

$$p = \rho(r) \xi(x), \quad (4.28)$$

this can be written as:

$$\frac{\rho''}{\rho} + \frac{1}{r} \frac{\rho'}{\rho} + \frac{\xi''}{\xi} + k^2 = 0 \quad (4.29)$$

Solutions:

$$\xi = \exp(-i\alpha x), \quad (4.30)$$

$$\rho = J_0(\epsilon r), \quad (4.31)$$

such that the solution for the pressure is:

$$p = J_0(\epsilon r) \exp(\alpha x) \quad (4.32)$$

under the condition:

$$\alpha^2 = k^2 - \epsilon^2. \quad (4.33)$$

At  $r = R$  we have the boundary condition that  $Z_0 \zeta_R u = p$ . After filling in and using the rule  $J_0'(x) = -J_1(x)$ :

$$\epsilon R \frac{J_{-1}(\epsilon R)}{J_0(\epsilon R)} = -iv, \quad (4.34)$$

where  $v = \frac{kR}{\zeta_R}$ . This is the characteristic equation for  $\epsilon R$ . Solutions for

$$\epsilon \approx + \frac{1}{R} \sqrt{\frac{96 + 36iv \pm \sqrt{9216 + 2304iv - 912v^2}}{12 + iv}} \quad (4.35)$$

where  $0 \leq \Re[\epsilon R] \leq 2$  and  $0 \leq \Im[\epsilon R] \leq 3$  should be satisfied in order to guarantee precision, see Mechel, p. 630.

#### 4.5 Prismatic duct with flow

- Assuming fully developed plug flow in a duct the linearized governing equations in frequency domain read:

$$i\omega \rho + \rho_0 \frac{du}{dx} + u_0 \frac{d\rho}{dx} = 0 \quad (4.36)$$

$$i\rho_0 \omega u + \rho_0 u_0 \frac{du}{dx} + \frac{dp}{dx} = 0 \quad (4.37)$$

$$p = c_0^2 \rho \quad (4.38)$$

- With subscript 0 are the mean flow variables. Eliminating  $\rho$ :

$$\frac{1}{c_0^2} \left( i\omega p + u_0 \frac{dp}{dx} \right) + \rho_0 \frac{du}{dx} = 0 \quad (4.39)$$

$$\rho_0 \left( i\omega u + u_0 \frac{du}{dx} \right) + \frac{dp}{dx} = 0 \quad (4.40)$$

- Taking spatial derivative of momentum and subtracting the convective derivative of the continuity equation from it yields the convective wave equation:

$$\left( i\omega + u_0 \frac{d}{dx} \right)^2 \frac{1}{c_0^2} p - \frac{d^2 p}{dx^2} = 0 \quad (4.41)$$

For constant  $u_0$ , we try solutions of the form:

$$p = A \exp(\alpha x), \quad (4.42)$$

which yields the characteristic equation for  $\alpha$ :

$$\underbrace{(M^2 - 1)}_a \alpha^2 + \underbrace{2Mki}_b \alpha - \underbrace{k^2}_c = 0, \quad (4.43)$$

where  $M$  denotes the Mach number  $u_0/c_0$ . The solutions for  $\alpha$  are:

$$\alpha = i \frac{Mk \pm k}{1 - M^2} = \pm ik \frac{1}{1 \mp M} \quad (4.44)$$

Written out:

$$p = A \exp\left(-\frac{ik}{1+M}x\right) + B \exp\left(\frac{ik}{1-M}x\right), \quad (4.45)$$

and the volume flow:

## 4.6 Cremers impedance

$$\frac{kR}{\zeta} = 2.9803824 + 1.2796025i \quad (4.46)$$

Or:

$$\zeta = kR(0.28 - 0.12i) \quad (4.47)$$

Attenuation reached when the liner impedance equals Cremer's impedance is around 15 dB per unit of radius maximum. It decreases with increasing frequency, when  $fR \approx 100$ .

### 4.6.1 Locally reacting lining with back-volume

Impedance of concentric liner, outer radius is  $R_o$ , inner radius is  $R_i$

$$\zeta_{\text{back}} = i \frac{H_0^{(1)}(kR_i) - \frac{H_1^{(1)}(kR_o)}{H_1^{(2)}(kR_o)} H_0^{(2)}(kR_i)}{H_1^{(1)}(kR_i) - \frac{H_1^{(1)}(kR_o)}{H_1^{(2)}(kR_o)} H_1^{(2)}(kR_i)} \quad (4.48)$$

Such that the total impedance is

$$\zeta = \zeta_{\text{back}} + \zeta_{\text{MPP}} \quad (4.49)$$

## 4.7 Cavity silencer

-

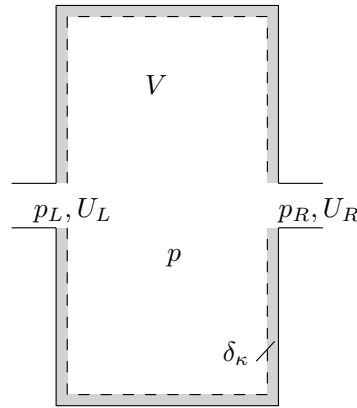


Figure 4.3 – Schematic of the compliance volume segment.

## 4.8 Compliance volume

Figure 4.3 gives a schematic of the compliance volume. A compliance volume is implemented in the LRFTubes code in the Volume class. A compliance volume is a volume (tank) which is small compared to the wavelength. Hence, we can assume that the acoustic pressure is constant throughout the volume  $V$ . As thermal relaxation still occurs, the model for this segment takes into account thermal relaxation due to temperature oscillations. The basic assumptions behind the model are:

- The characteristic length scale of volume is small compared to the wavelength.
- The characteristic length scale of volume is large compared to thermal penetration depth.

The lower the frequency, the more the second assumption is violated, while the higher the frequency, the more the first assumption is violated. In practice, violating the first assumption has a larger impact. For a compliance, the following governing equations can be derived [15, p. 156]:

$$p_L = p = p_R, \quad (4.50)$$

$$U_R = U_L - i\omega C_c p, \quad (4.51)$$

in which  $C_c$  is the acoustic “capacitance”:

$$C_c = \frac{1}{z_0 c_0} \left( V + \frac{1}{2} \frac{(1-i)(\gamma-1)}{1+\epsilon_{s,0}} S \delta_\kappa \right) \quad (4.52)$$

where  $V$  is the volume,  $S$  the surface area of the volume in contact with a wall, and

$$\epsilon_{s,0} = \sqrt{\frac{\kappa \rho_0 c_p}{\kappa_s \rho_s c_s}}. \quad (4.53)$$

It should be noticed that in practice, a compliance volume often functions as the end of an acoustic system. In that case, either  $U_L$  or  $U_R$  is 0.

## 4.9 Membrane

A membrane is a mechanical

## 4.10 Hole

`series_impedance.py/class CircHoleNeck(SeriesImpedance)`

Behaves like an acoustic mass with losses. It represents holes in sheet material, which can form the neck of a Helmholtz resonator. Hole-hole interaction is neglected. The resistance term is an approximation.

Usable for connecting volumes to each other or volumes to ducts, to form Helmholtz resonators.

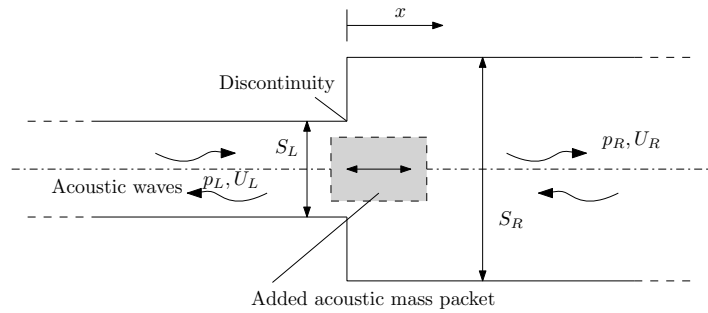


Figure 4.4 – Schematic of a waveguide discontinuity.

#### 4.11 End corrections and discontinuities

For discontinuities in the cross section of a waveguide, and the case of inviscid adiabatic wave propagation, an exact expression is available for the added acoustic mass [6]. Figure 4.4 gives a schematic of the situation. The model is implemented in the `Discontinuity` class in the `LRFTubes` code. The assumptions behind the model are:

- Both tubes on either side of the discontinuity are cylindrical. The tubes are co-axially connected.
- The wavelength is larger than transverse characteristic length scale.
- Other discontinuities are far away from the current one.
- Inviscid and adiabatic wave propagation (Helmholtz equation).

The ratio of tube radii  $a_L/a_R$  is denoted by  $\alpha$ . It turns out that a surface area discontinuity only generates an acoustic pressure discontinuity. The volume flow is preserved. Hence:

$$U_R = U_L \quad (4.54)$$

$$p_R = p_L - i\omega M_A U_L \quad (4.55)$$

where  $M_A$  is the so-called added acoustic mass in  $\text{kg}\cdot\text{m}^{-4}$ , which equals

$$M_A = \chi(\alpha, k) \frac{8\rho_0}{3\pi^2 a_L}, \quad (4.56)$$

where  $\chi$  is Karal's discontinuity factor, which is in general a function of the tube radii and the wave number. For  $\lambda \gg a_R$ , the dependency of  $\chi$  on the wave number  $k$  can be neglected, which lowers the computational burden significantly, as  $\chi$  has to be computed only once. For the case  $\alpha \rightarrow 0$  (by letting  $a_R \rightarrow \infty$ ),  $\chi \rightarrow 1$ . In case of  $\alpha \rightarrow 1$ , the acoustic mass gradually reduces to zero as  $\chi \rightarrow 0$ . When  $\alpha = 1$ , there is no continuity left, such that  $M_A = 0$ .

The derivation of the coefficient  $\chi$  is documented in Appendix B, except of the following information. To solve the curve of  $\chi$ , a system of infinite equations has to be solved for an infinite number of unknowns. In the `LRFTubes` code, as a standard this system is truncated up to  $N = 100$  equations and 100 unknowns. Figure 4.5 shows the effect of truncating this infinite system of equations. As visible for the case of 100 equations, the curves start to deviate from each other for lower values of  $\alpha$ . Assuming that convergence is obtained as  $N \rightarrow \infty$ , the curve of  $N = 100$  has acceptable accuracy for  $\alpha > 0.07$ . To limit possible faulty results, the `LRFTubes` code gives a warning when the tube ratio is chosen such that an invalid  $\chi$  is computed. When an  $\alpha < 0.07$  is desired, the user should choose a higher value of  $N$ .

#### 4.12 Hard wall

A hard wall is the wall perpendicular to the wave propagation direction. Figure 4.6 shows the schematic configuration for this segment. Due to thermal relaxation a hard wall consumes acoustic energy is consumed. The hard wall segment models this thermal relaxation loss. The assumptions behind the model are:

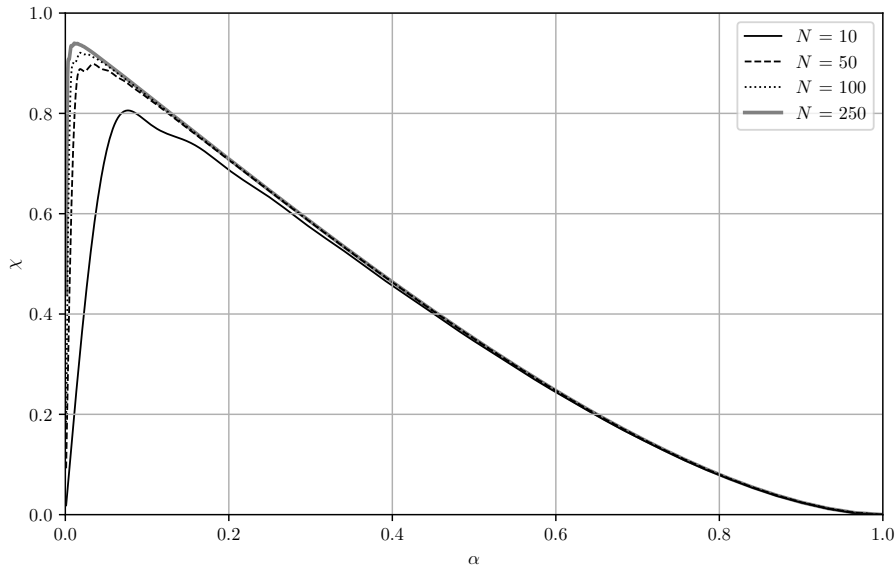


**Figure 4.5** –  $\chi$  vs  $\alpha$  for different truncations ( $N$ ) of the infinite system of equations.

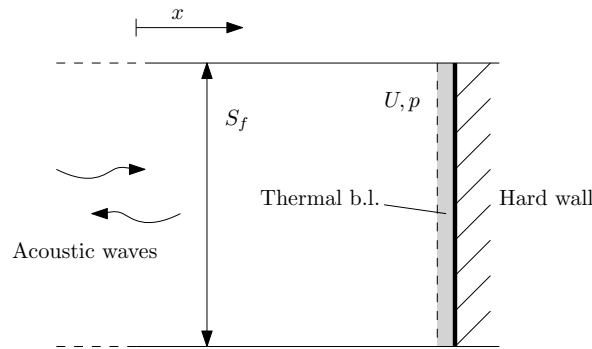


**Figure 4.6** – Schematic of a hard acoustic wall where the thermal boundary layer dissipates a bit of the acoustic energy ( $Z \neq \infty$ ).

- Normal incident waves.
- Uniform normal velocity.
- The wavelength is much larger than the thermal penetration depth ( $\lambda \gg \delta_\kappa$ ).

We can derive the following impedance boundary condition [15, p. 157]:

$$U = k\delta_\kappa \frac{S}{z_0} \frac{(\gamma - 1)(1 + i)}{2(1 + \epsilon_s)} p. \quad (4.57)$$

Hence the impedance of a hard wall scales with  $Z \sim Z_0 \frac{\lambda}{\delta_\kappa}$ . For 1 kHz, this results in  $\sim 4100Z_0$ , which is practically already close to  $\infty$ . Except for really high frequencies this segment can often be replaced with a boundary condition of  $U = 0$ . An important point to make here is that this boundary condition is inconsistent with the LRF solution for 1D wave propagation in ducts, as the velocity profile in a duct is not uniform. This is especially true for the case of small ducts where  $r_h \sim \delta$ .

### 4.13 Spherical wave propagation models

For spherical waves, the Helmholtz equation reads

$$\left( \frac{d^2}{dr^2} + \frac{2}{r} \frac{d}{dr} + \Gamma^2 \right) p = 0. \quad (4.58)$$

The solution of Eq. 4.58 reads:

$$p = \frac{C_1 \exp(-i\Gamma r) + C_2 \exp(i\Gamma r)}{r}. \quad (4.59)$$

The acoustic volume flow can be computed as

$$U = i \frac{\alpha 4\pi r^2}{\Gamma z_c} \frac{dp}{dr}, \quad (4.60)$$

where  $\alpha = 1$  for a full sphere and  $\alpha = \frac{1}{2}$  for a hemisphere. We can derive the following transfer matrix for  $p$  and  $U$ :

$$\begin{Bmatrix} p \\ U \end{Bmatrix}_R = \begin{bmatrix} M_{11} & M_{12} \\ M_{21} & M_{22} \end{bmatrix} \begin{Bmatrix} p \\ U \end{Bmatrix}_L, \quad (4.61)$$

where

$$M_{11} = \frac{r_L}{r_R} \cos(\Gamma(r_L - r_R)) - \frac{1}{\Gamma r_R} \sin(\Gamma(r_L - r_R)), \quad (4.62)$$

$$M_{12} = \frac{iz_c \sin(\Gamma(r_L - r_R))}{4\pi\alpha r_L r_R}, \quad (4.63)$$

$$M_{21} = \frac{4\pi i\alpha}{z_c} \left[ \left( r_L r_R + \frac{1}{\Gamma^2} \right) \sin(\Gamma(r_L - r_R)) + \frac{r_R - r_L}{\Gamma} \cos(\Gamma(r_L - r_R)) \right] \quad (4.64)$$

$$M_{22} = \frac{r_R}{r_L} \cos(\Gamma(r_L - r_R)) + \frac{1}{\Gamma r_L} \sin(\Gamma(r_L - r_R)), \quad (4.65)$$

### 4.14 Boundary conditions

#### 4.14.1 Radiation impedance of a baffled piston

- $a$ : radius of the exit [m]
- $S$ :  $\pi a^2$

$$p = Z_{\text{rad}} U, \quad (4.66)$$

$$Z_{\text{rad}} = \frac{z_0}{S} \left[ 1 - \frac{2J_1(2ka)}{2ka} + i \frac{2H_1(2ka)}{2ka} \right] \quad (4.67)$$

In the low frequency range, a power series expansion of  $H_1$  yields [Aarts]:

$$H_1(x) = \frac{2}{\pi} \left[ \frac{x^2}{3} - \frac{x^4}{45} + \frac{x^6}{1575} - \dots \right] \quad (4.68)$$

Filling this in, we obtain the following low-frequency approximation to  $Z_{\text{rad}}$ :

$$Z_{\text{rad}} = \frac{z_0}{S} \left[ i \frac{8ka}{3\pi} + \frac{1}{2} (ka)^2 + \mathcal{O}((ka)^3) \right] \quad (4.69)$$

# Chapter 5

## Speaker

### 5.1 As an active element, with voltage control

The speaker generates electromotive force

$$F_{\text{emf}} = BlI, \tag{5.1}$$

where  $Bl$  is the “motor constant”, or force factor, in units  $\text{N} \cdot \text{A}^{-1}$ , or  $\text{V} \cdot \text{s} \cdot \text{m}^{-1}$ . The back-emf “force”:

$$V_{\text{bemf}} = Blu \tag{5.2}$$

The “circuit equation”:

$$V_{\text{in}} - V_{\text{bemf}} = Z_{\text{el}}I, \tag{5.3}$$

where  $Z_{\text{el}}$  is the equivalent impedance of the electrical circuit in  $\Omega$ . The mechanical impedance comprises a stiffness part, a damping part and a mass part. The equation of motion is:

$$z_m u = F_{\text{emf}} + p_l S - p_r S, \tag{5.4}$$

where  $u$  denotes the velocity phasor of the membrane. The mechanical impedance  $z_m$  is defined as:

$$z_m = i\omega m_m + r_m + \frac{k_m}{i\omega}, \tag{5.5}$$

where  $m_m$  is the moving mass,  $r_m$  the damping force and  $k_m$  the spring constant.  $z_m$  can equivalently be written as:

$$z_m = m \left( i\omega + 2\zeta\omega_r + \frac{\omega_r^2}{i\omega} \right), \tag{5.6}$$

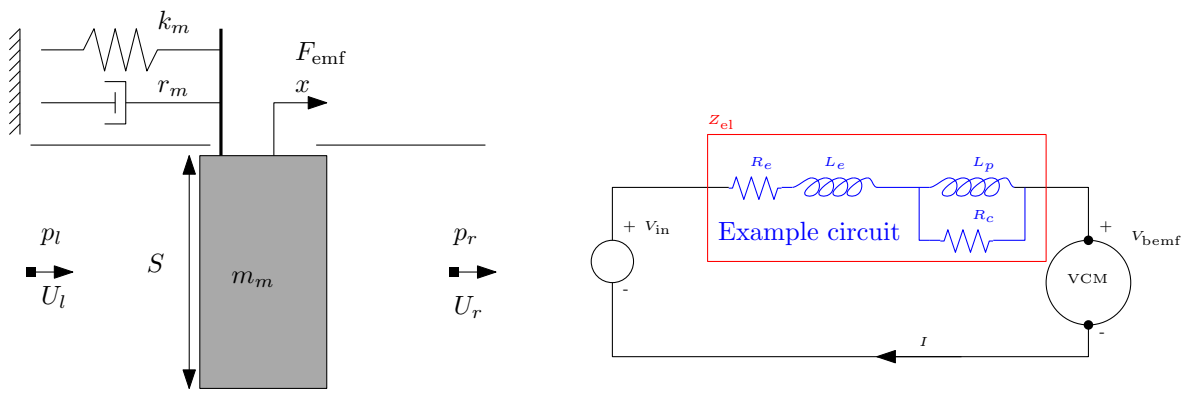


Figure 5.1 – Electrical and mechanical model of the speaker

where

$$\omega_r^2 = \frac{k_m}{m_m} \quad ; \quad \zeta = \frac{r_m}{2\sqrt{k_m m_m}} = \frac{r_m}{2\omega_r m_m} = \frac{\omega_r r_m}{2k_m}. \quad (5.7)$$

After some algebraic manipulations we find:

$$\frac{1}{S_l} \left( z_m + \frac{(B\ell)^2}{Z_{el}} \right) U_l = p_l S_l - p_r S_r + \frac{B\ell}{Z_{el}} V_{in}, \quad (5.8)$$

$$U_r - U_l = 0, \quad (5.9)$$

which is in transfer matrix notation:

$$\begin{Bmatrix} p_r \\ U_r \end{Bmatrix} = \mathbf{T} \begin{Bmatrix} p_l \\ U_l \end{Bmatrix} + \mathbf{s}, \quad (5.10)$$

where

$$\mathbf{T} = \begin{bmatrix} 1 & -\frac{1}{S^2} \left( z_m + \frac{(B\ell)^2}{Z_{el}} \right) \\ 0 & 1 \end{bmatrix} \quad ; \quad \mathbf{s} = \begin{Bmatrix} \frac{B\ell}{Z_{el} S} V_{in} \\ 0 \end{Bmatrix} \quad (5.11)$$

## 5.2 As antireciprocal segment

As antireciprocal segment, a voltage controlled speaker has electrical connections on the left side, and acoustic connections on the right side:

$$\begin{Bmatrix} p \\ U \end{Bmatrix}_R = \mathbf{T}_{\text{spk}} \begin{Bmatrix} V \\ I \end{Bmatrix}_L. \quad (5.12)$$

A model us used for the back cavity pressure build-up which can be added as an extra impedance, placed in series with the effective acoustic impedance of the front side, hence the force balance reads:

$$F_{\text{emf}} = Z_{\text{back}} U + Z_{\text{front}} U \quad (5.13)$$

The transfer matrix reads:

$$\mathbf{T}_{\text{spk}} = \begin{bmatrix} -\frac{S^2 Z_{\text{back}} + z_m}{SB\ell} & \frac{(B\ell)^2 + Z_{el}(z_m + S^2 Z_{\text{back}})}{B\ell S} \\ \frac{S}{B\ell} & -\frac{SZ_{el}}{B\ell} \end{bmatrix} \quad (5.14)$$

For a closed back-cavity volume, the back-cavity is:

Then again:

## Chapter 6

# Optimized reactive silencers

### 6.1 Parallel Helmholtz resonator transfer function and transmission loss

Equations for a side branch Helmholtz resonator:

$$p_R = p_L, \quad (6.1)$$

$$U_R = U_L - p_L/Z_h, \quad (6.2)$$

where  $Z_h$  is the side branch impedance of the Helmholtz resonator, defined as

$$Z_h = \left( \frac{\rho_0 z_0}{i\omega V} + R_v + i\omega m_{\text{neck}} \right), \quad (6.3)$$

where

$$m_{\text{neck}} = \frac{\rho_0 \ell_{\text{eff,neck}}}{S_{\text{neck}}}, \quad (6.4)$$

and for relatively large holes, air at STP, the resistance term can be estimated as:

$$R_v \approx 7.2 \times 10^{-3} z_0/S_h, \quad (6.5)$$

Now, the following substitutions are made:

$$C = \frac{V}{\rho_0 z_0}, \quad (6.6)$$

$$m_{\text{neck}} = \frac{1}{\omega_r^2 C} \quad (6.7)$$

$$\zeta = \frac{1}{2} \omega_r C R_v. \quad (6.8)$$

such that we can write:

$$Z_h = \frac{1}{\omega_r C} \left( \frac{\omega_r}{i\omega} + 2\zeta + \frac{i\omega}{\omega_r} \right) \quad (6.9)$$

The quality factor of the resonator is the ratio of the resonance frequency to its bandwidth measure. If we take

$$Q \stackrel{\text{def}}{=} \frac{f_r}{\Delta f}, \quad (6.10)$$

where  $\Delta f$  is the full width at half the maximum value, i.e. the frequency distance between two points lying at  $-3$  dB w.r.t. the maximum value. The damping ratio  $\zeta$  is related to  $Q$  as:

$$\zeta = \frac{1}{2Q} = \frac{1}{2} \frac{\Delta f}{f_r} \quad (6.11)$$

Assembling the transfer matrix

$$\begin{Bmatrix} p \\ U \end{Bmatrix}_R = \begin{bmatrix} T_{11} & T_{12} \\ T_{21} & T_{22} \end{bmatrix} \begin{Bmatrix} p \\ U \end{Bmatrix}_L, \quad (6.12)$$

where

$$T_{11} = 1 \quad (6.13)$$

$$T_{12} = 0 \quad (6.14)$$

$$T_{21} = -Z_h^{-1} \quad (6.15)$$

$$T_{22} = 1 \quad (6.16)$$

### 6.1.1 Transmission loss

The transmission coefficient can be computed as:

$$\tau = \frac{C}{A} = \frac{Z_0 (T_{21}p_L + T_{22}U_L)}{\frac{1}{2} (p_L + Z_0U_L)}, \quad (6.17)$$

using

$$T_{11}p_L + T_{12}U_L = p_R = Z_0U_R = Z_0 (T_{21}p_L + T_{22}U_L), \quad (6.18)$$

we get

$$U_L = \frac{(T_{11} - Z_0T_{21})}{(Z_0T_{22} - T_{12})} p_L, \quad (6.19)$$

filling in:

$$\tau = \frac{2}{Z_0} \frac{T_{11}T_{22} - T_{12}T_{21}}{T_{11} - T_{12}/Z_0 - T_{21}Z_0 + T_{22}}, \quad (6.20)$$

assuming that the determinant of the transfer matrix be unity ( $T_{11}T_{22} - T_{12}T_{21} \equiv 1$ ), this can be further simplified:

$$\tau = \frac{2}{T_{11} - T_{12}/Z_0 - T_{21}Z_0 + T_{22}}, \quad (6.21)$$

For a Helmholtz resonator, this results in:

$$\tau(\omega) = \frac{2Z_h(\omega)}{Z_0 + 2Z_h(\omega)}, \quad (6.22)$$

Filling in the Helmholtz resonator equation:

$$\tau(\omega) = \frac{2 \left( 1 + 2 \frac{\omega}{\omega_r} \zeta - \left( \frac{\omega}{\omega_r} \right)^2 \right)}{2 \left( 1 + 2 \frac{\omega}{\omega_r} \zeta - \left( \frac{\omega}{\omega_r} \right)^2 \right) + i \frac{\omega}{\omega_r} \left( \frac{Cz_0\omega_r}{S} \right)} \quad (6.23)$$

The peak height, filling in for  $\omega/\omega_r = 1$ :

$$\tau = \frac{4\zeta}{4\zeta + \beta}, \quad (6.24)$$

where  $\beta$  is defined as the resonator strength:

$$\beta = \frac{V\omega_r}{Sc_0} \quad (6.25)$$

In terms of transmission loss:

$$TL_{\omega=\omega_r} = 20 \log \left( \frac{\beta + 4\zeta}{4\zeta} \right) \quad (6.26)$$

The peak half width is the distance over which the transmission loss has dropped 3 dB w.r.t. the transmission loss at the resonance frequency. This is an important design parameter. We can compute it by setting

$$\left| \frac{\tau|_{\omega_r+\Delta\omega}}{\tau|_{\omega_r}} \right| = \sqrt{2}, \quad (6.27)$$

For light relative damping, and  $\Delta\omega/\omega_r \approx 1$ ,

$$\left| \frac{\tau|_{\omega_r+\Delta\omega}}{\tau|_{\omega_r}} \right| \approx \frac{\alpha - 1}{\zeta}, \quad (6.28)$$

So given the -3 dB point, and the maximum required transmission loss, we can compute  $\zeta$  and  $\beta$ :

- $\zeta = \frac{\alpha_{-3dB} - 1}{\sqrt{2}}$
- $\beta = 4\zeta \left( 10^{\frac{TL_{max}}{20}} - 1 \right)$

Required volume in terms of resonator strength:

$$V = \frac{Sc_0\beta}{\omega_r} \quad (6.29)$$

### 6.1.2 Insertion loss

For computation of the insertion loss, we require two more parameters:

- The load impedance at the downstream end of the silencer
- The output impedance of the source ( $Z_{rad}$ )

Suppose the source strength is defined by  $\mathcal{S}$ . Situation without silencer:

$$U_L = \mathcal{S}/(Z_s + Z_l), \quad (6.30)$$

$$U_R = U_L, \quad (6.31)$$

$$p_R = Z_{rad}U_R, \quad (6.32)$$

where  $Z_s$  denotes the source output impedance, and  $Z_l$  denotes the load impedance as felt by the source.

For the reference case, the load impedance equals the radiation impedance, and the radiated acoustic power is:

$$P_{ref} = \frac{1}{2} \frac{|\mathcal{S}|^2}{|Z_{rad} + Z_s|^2} \Re [Z_{rad}] \quad (6.33)$$

Now, situation including silencer, with in general, transfer matrix  $T$ .

$$P_{with\ silencer} = \frac{1}{4} |\mathcal{S}|^2 \frac{\Re [Z_{rad}]}{|T_{22}Z_{rad} - T_{12} + Z_s (T_{11} - T_{21}Z_{rad})|^2} \quad (6.34)$$

From that, computing the power ratio, that  $\det T \equiv 1$  for a reciprocal system:

$$R_P = \frac{P_{with\ silencer}}{P_{ref}} = \frac{|Z_{rad} + Z_s|^2}{|T_{22}Z_{rad} - T_{12} + Z_s (T_{11} - T_{21}Z_{rad})|^2} \quad (6.35)$$

### 6.1.3 Insertion loss for a Helmholtz side branch resonator

Filling in for a simple Helmholtz side branch resonator:

$$R_{P,\text{Helmholtz}} = \frac{|Z_{\text{rad}} + Z_s|^2}{|Z_{\text{rad}} + Z_s \left(1 + \frac{Z_{\text{rad}}}{Z_h}\right)|^2}. \quad (6.36)$$

Comparing this to the transmission loss curve:

$$|\tau|_{\text{Helmholtz}}^2 = \frac{4|Z_h|^2}{|2Z_h + Z_0|^2} \quad (6.37)$$

#### 6.1.3.1 High output impedance limit ( $Z_s \gg Z_{\text{rad}}$ ), volume flow source

$$R_{P,\text{Helmholtz}} = \frac{|Z_h|^2}{|Z_h + Z_{\text{rad}}|^2}. \quad (6.38)$$

#### 6.1.3.2 Low output impedance limit ( $Z_s \ll Z_{\text{rad}}$ ), pressure source

$$R_{P,\text{Helmholtz}} = \frac{|Z_h|^2}{|Z_h + Z_s|^2} \quad (6.39)$$

#### 6.1.3.3 Special case: barrier in an infinite space ( $Z_s = Z_{\text{rad}}$ )

$$R_{P,\text{Helmholtz}} = \frac{|Z_h|^2}{|Z_h + \frac{1}{2}Z_{\text{rad}}|^2}. \quad (6.40)$$

Comparing limits to power transmission ratio

$$|\tau|^2 = \frac{|Z_h|^2}{|Z_h + \frac{1}{2}Z_0|^2}, \quad (6.41)$$

So the transmission loss is the reduction in transmitted sound power for the situation where the source output impedance equals the radiation impedance on the other side of the silencer.

### 6.1.4 Multiple Helmholtz resonators at a single inlet

In case multiple resonators are connected to the same inlet, the parallel impedance can be computed by computing the equivalent parallel impedance:

$$\frac{1}{Z_{h,\text{tot}}} = \frac{1}{Z_{h,1}} + \frac{1}{Z_{h,2}} + \dots \quad (6.42)$$

## 6.2 Transmission of the duct

$$\begin{Bmatrix} p_R \\ U_R \end{Bmatrix} = \begin{bmatrix} \cos(kL) & -iZ_0 \sin(kL) \\ -iZ_0^{-1} \sin(kL) & \cos(kL) \end{bmatrix} \begin{Bmatrix} p_L \\ U_L \end{Bmatrix} \quad (6.43)$$

## Chapter 7

# (Micro)-perforated plate design

Given  $\beta$ ,  $\zeta$  and  $\omega_r$ , a proper acoustic mass has to be chosen. Given the resonator equations, the viscous resistance and required acoustic mass can be determined. This results in requirements for the (effective) acoustic mass and resistance of the perforate. For arbitrary hole sizes, the definition of the acoustic impedance of a perforate is:

$$z = \frac{\Delta p}{\bar{u}}. \quad (7.1)$$

where  $\bar{u}$  denotes the acoustic volume flow per unit of area through the perforate (uncorrected yet for porosity), such that the area-averaged velocity *in a hole* is  $u_h = \bar{u}/\phi$ , where  $\phi$  denotes the porosity. In Eq. 7.1, it is assumed that the acoustic wavelength is typically much larger than the length scale(s) of the perforate. The model for the impedance of a perforate, in the linear range is :

$$z = \frac{i\omega\rho_0}{\phi} \left[ \frac{t_w}{(1-f_v)} + 2\delta f_{\text{int}} \right] + \alpha \frac{\rho_0\omega\delta_v}{\phi}, \quad (7.2)$$

where  $f_{\text{int}}$  is the hole-hole interaction function which  $\rightarrow 1$  for  $\phi \rightarrow 0$ , and  $\delta$  is the single-sided hole (therefore, the factor 2 in front) end correction due to the added mass effect, for the situation of negligible hole-hole interaction. [Paper: Tayong, 2013].

$$f_{\text{int}}(\phi) = 1 - 1.4092\sqrt{\phi} + 0.33818\sqrt{\phi}^3 + 0.06793\sqrt{\phi}^5. \quad (7.3)$$

$$- 0.02287\sqrt{\phi}^6 + 0.063015\sqrt{\phi}^7 - 0.01614\sqrt{\phi}^8 \quad (7.4)$$

For square holes:

where

$$\xi^2 = \frac{\pi D^2}{4P^2} \quad (7.5)$$

$$\frac{D}{P} = \sqrt{\frac{4\phi}{\pi}}. \quad (7.6)$$

For circular large holes with diameter  $D$ , the end correction for both sides is

$$2\delta = \frac{8}{3\pi}D \approx 0.85D. \quad (7.7)$$

For circular large holes with diameter  $D$ , the end correction for both sides is

$$2\delta = \frac{8}{3\pi}D \approx 0.85D. \quad (7.8)$$

Here we use a more advanced model, which includes the shear wave number. For unrounded edges and a perforate thickness of  $t_p$ , the added mass end correction can be computed as:

$$2\delta = \frac{1}{2} \left[ 0.97 \exp\left(-0.14 \frac{D}{\delta_v}\right) + 1.54 - 0.003 \frac{D}{t_p} \right] D \quad (7.9)$$

The factor  $\alpha$

$$\alpha = 5.08 \left( \frac{D}{\sqrt{2}\delta_v} \right)^{-1.45} + 1.70 - 0.002 \frac{D}{t_p}. \quad (7.10)$$

## 7.1 Tuning the hole diameter for large holes and the negligible hole-hole interaction

The coarse impedance of a Helmholtz resonator repeated here:

$$Z(\omega) = \underbrace{i\omega m_A + R_v}_{Z_h} + \frac{\rho_0 c_0^2}{i\omega V}, \quad (7.11)$$

The resistive and reacting part  $i\omega m_A + R_v$  is due to the resonator holes,

$$Z_h = i\omega m_A + R_v \approx \frac{1}{S} \left[ \frac{i\omega \rho_0}{\phi} \left[ \frac{t_w}{(1-f_v)} + 2\delta f_{\text{int}} \right] + \frac{\alpha \rho_0 \omega \delta_v}{\phi} \right]. \quad (7.12)$$

In the large hole limit, or high shear wave number:

$$\Re [i\omega m_A + R_v] \approx \frac{\rho_0 \delta_v \omega}{\phi S} \left[ \alpha + \frac{2t_w}{(D-4\delta_v)} \right] \underbrace{\propto}_{\text{approx.}} \sqrt{\omega}.$$

In the large hole limit, without hole-hole interaction and  $\delta_v \rightarrow 0$ , we the resonance frequency of the system is:

$$\omega_{r,\text{lh}}^2 = \frac{\phi S c_0^2}{V (1.54D + t_w)} \quad (7.13)$$

–

$$Z_{\text{large holes, res}}(\omega) = \frac{c_0^2 \rho_0}{V \omega_{r,\text{lh}}^2} \left[ \frac{\omega_{r,\text{lh}}^2}{i\omega} + \frac{i\omega t_w}{\left\{ 1 + 2 \frac{\delta_v(i-1)}{D} \right\} (2\delta f_{\text{int}} + t_w)} + \frac{i\omega [2\delta f_{\text{int}} - i\delta_v \alpha]}{2\delta f_{\text{int}} + t_w} \right] \quad (7.14)$$

### 7.1.1 COMSOL boundary condition to useful

When using COMSOL to compute Helmholtz resonances, the added mass effect is included just by solving the Helmholtz equation. Therefore, to model the holes, only the final wall thickness part of the added mass (and hole-hole interaction), and the resistive part of the impedance should be added to the simulation. If we look at Eq. 7.12, it means only the following part:

$$z_{\text{bc, COMSOL}} = i\omega \rho_0 \frac{t_w}{1-f_v} + \alpha \rho_0 \omega \delta_v. \quad (7.15)$$

### 7.1.2 Porosity estimator constraint

An estimation for the porosity is a good requirement, as a too large porosity leads to too much hole-hole interaction and shift away from proper Helmholtz resonators. First of all, we set the surface area at the inner duct, which is available for holes as

$$S = \Pi L_h, \quad (7.16)$$

and we fix  $L_h$  to

$$L_h = \lambda_r/20 = \frac{2\pi c_0}{20\omega_{r,\text{lh}}} = \frac{\pi c_0}{10\omega_{r,\text{lh}}}. \quad (7.17)$$

Rewriting Eq. 7.13 to  $\phi$  yields:

$$\phi_{\text{estimation}} \approx \frac{10}{\pi} \frac{V(1.54D + t_w) \omega_{r,\text{lh}}^3}{\Pi c_0^3} \leq 0.1 \quad (7.18)$$

See what this constraint does...\*

## 7.2 Large hole (boundary layer) limit

$$\phi = \frac{S_{\text{hole}}}{S_{\text{tot}}} \quad (7.19)$$

$\delta_v \ll D$ . Given  $\zeta$  and  $\omega_r$ . Note that:

$$\zeta = \frac{1}{2} \frac{R}{m_A \omega_r} \approx \frac{1}{2} \frac{\Re[z]}{\Im[z]} \quad (7.20)$$

Procedure:

In the boundary layer limit:

$$f_v = \frac{(1-i)\delta_v}{2r_h}, \quad (7.21)$$

such that:

$$z_{\text{perforate}} = \frac{i\omega\rho_0}{\phi} \frac{t_w + 2\delta f_{\text{int}}}{\left(1 - \frac{\delta_v}{2r_h} + \frac{i\delta_v}{2r_h}\right)} \quad (7.22)$$

Typical resistance: fill in  $\omega = \omega_r$ . Filling in:

$$\zeta \approx \frac{\delta_v}{D}. \quad (7.23)$$

The real part of the perforate impedance is the resistive part. In a 3D simulation, this impedance can be added to a surface of the hole, to model the hole *resistance* in an otherwise inviscid simulation. The real part is:

$$(7.24)$$

### 7.2.1 Lots of holes

Hereby, once we know the hole diameter, the required acoustic mass can be tuned using the porosity:

$$m_A \approx \frac{\Im[z(\omega = \omega_r)]}{\omega S_t} \approx \frac{1}{S_{\text{tot}}\phi} \left( \frac{\rho_0 8D f_{\text{int}}(\phi)}{3\pi} + \rho_0 t_w \right) \quad (7.25)$$

So that the porosity can be computed as:

$$\phi \approx F(\phi) = \frac{D\rho_0(D - 2\delta_v)(8Df_{\text{int}} + 3\pi t_w)}{3\pi S_{\text{tot}} m_A (D^2 - 4D\delta_v + 8\delta_v^2)} \approx \frac{\rho_0(8Df_{\text{int}}(\phi) + 3\pi t_w)}{3\pi S_{\text{tot}} m_A}. \quad (7.26)$$

Note that this is a transcendental equation in  $\phi$ , which can easily be solved by iterating  $\phi$ :

$$\phi_1 = F(1) \quad (7.27)$$

$$\phi_2 = F(\phi_1) \quad (7.28)$$

$$\phi_3 = F(\phi_2) \quad (7.29)$$

$$\vdots = \vdots \quad (7.30)$$

### 7.2.2 Some holes

For only “some holes”, far away from each other, we fill in for  $\phi = \frac{1}{4} N_{\text{hole}} \pi D^2 / S_{\text{tot}}$ :

$$m_A \approx \frac{\rho_0}{3\pi N_{\text{hole}} D} \left( \frac{32}{\pi} + \frac{12t_w}{D} \right) \quad (7.31)$$

So the number of holes can be chosen as:

$$N_{\text{holes}} \approx \frac{4\rho_0 (8Df_{\text{int}} + 3\pi t_w)}{3\pi^2 D^2 m_A} \quad (7.32)$$

### 7.3 Small hole limit

In the small hole limit,

$$f_v \approx 1 - \frac{iD^2}{16\delta_v^2} \quad (7.33)$$

Such that:

$$\zeta = \frac{1}{2} \frac{R}{m_A \omega_r} \approx \frac{1}{2} \frac{\Re [z(\omega = \omega_r)]}{\Im [z(\omega = \omega_r)]} \approx \frac{3\pi \delta_v^2 t_w}{D^3 f_{\text{int}}} \quad (7.34)$$

Such that:

$$D = \sqrt[3]{\frac{6\pi \delta_v^2 t_w}{6\zeta}}. \quad (7.35)$$

And:

$$m_A = \rho_0 \frac{8Df_{\text{int}}}{3\pi S_{\text{tot}} \phi} \quad (7.36)$$

Such that:

$$\phi \approx \rho_0 \frac{8Df_{\text{int}}}{3\pi S_{\text{tot}} m_A} \quad (7.37)$$

### 7.4 Geometry of hole patterns

For a square hole pattern, with hole-hole pitch  $P$ , the overall surface of a unit cell  $S_{\text{unit}} = P^2$ . For a certain porosity, the pitch can then be computed as:

$$P = \sqrt{\frac{\pi}{4\phi}} D. \quad (7.38)$$

For a hexagonal hole pattern (Fig. 7.1) with hole-hole pitch  $P$ , the overall surface of a unit cell  $S_{\text{unit}} = \frac{\sqrt{3}}{2} P^2$ . Henceforth, the pitch can be computed from the porosity and the hole diameter as:

$$P = \sqrt{\frac{\sqrt{3}\pi}{6\phi}} D. \quad (7.39)$$

The most important design parameters of a perforate are the porosity and the hole diameter.

### 7.5 Addition of acoustic hole resistance in an otherwise inviscid simulation

We assume that in a 3D FEM simulation, the imaginary acoustic impedance of a single hole

$$Z_{\text{hole}} = i\omega \rho_0 \frac{4}{\pi D^2} \left[ \frac{t_w}{(1-f_v)} + \frac{8Df_{\text{int}}}{3\pi C_D} \right], \quad (7.40)$$

$$\Re [z_{\text{hole}}] = \frac{2D\delta_v \omega \rho_0 t_w}{(4\delta_v^2 + (D - 2\delta_v)^2)}, \quad (7.41)$$

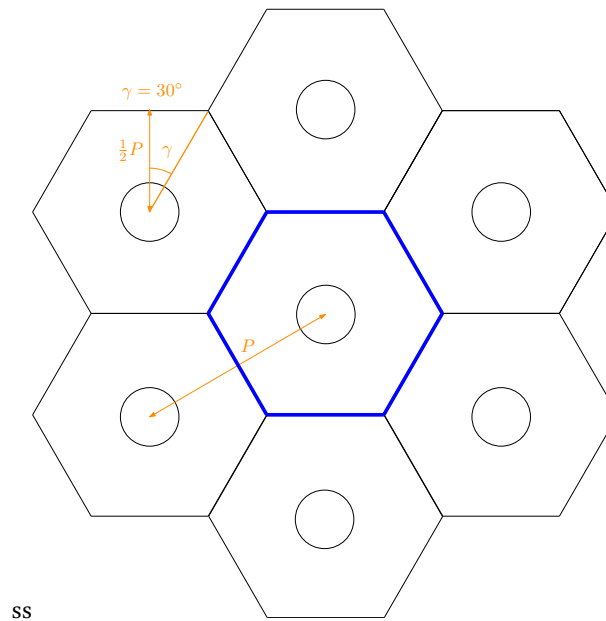


Figure 7.1 – Geometry details of a hexagonal hole pattern

## 7.6 Over-all transmission matrix

$$\begin{Bmatrix} p_R \\ U_R \end{Bmatrix}_1 = T_1 \begin{Bmatrix} p_L \\ U_L \end{Bmatrix}_1 \quad (7.42)$$

$$\begin{Bmatrix} p_R \\ U_R \end{Bmatrix}_2 = T_2 \begin{Bmatrix} p_R \\ U_R \end{Bmatrix}_1 \quad (7.43)$$

$$\begin{Bmatrix} p_R \\ U_R \end{Bmatrix}_3 = T_3 \begin{Bmatrix} p_R \\ U_R \end{Bmatrix}_2 \quad (7.44)$$

$$(7.45)$$

, hence

$$\begin{Bmatrix} p_R \\ U_R \end{Bmatrix}_3 = \underbrace{T_3 \cdot T_2 \cdot T_1}_T \begin{Bmatrix} p_L \\ U_L \end{Bmatrix}_1 \quad (7.46)$$

## **Chapter 8**

# **Miscellaneous models for acoustic components**

### **8.1 Acoustic impedance of small orifices**

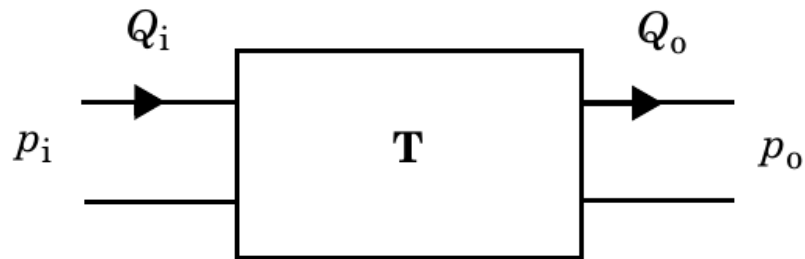
#### **8.1.1 Rectangular orifice**

#### **8.1.2 Slit orifice**

## Chapter 9

### Lookup model

LRFTubes allows importing transfer matrix data from externally computed sources (i.e. finite element model results). We focus on the use of COMSOL Multiphysics here. The output data from COMSOL should be created using the “Port Sweep” functionality. Implementation is only for 2 ports, as this is the only case for which COMSOL is able to export data. In COMSOL, the transfer matrix is defined as:



$$\begin{Bmatrix} p_i \\ Q_i \end{Bmatrix} = \begin{bmatrix} T_{11} & T_{12} \\ T_{21} & T_{22} \end{bmatrix} \begin{Bmatrix} p_o \\ Q_o \end{Bmatrix}, \quad (9.1)$$

hence the transfer matrix definition of LRFTubes is the *inverse* of the definition of COMSOL Multiphysics:

$$T_{\text{LRFTubes}} = T_{\text{COMSOL}}^{-1} \quad (9.2)$$

To properly use the Lookup model, in COMSOL port 1 should be corresponding to the LEFT side of a segment, and port 2 should be corresponding to the RIGHT side of a segment. Then, the data should be exported to a *txt* file with the columns in the following order: frequency, T11, T12, T21, T22. A file of this format, as exported by COMSOL can be passed to the constructor of *LookupModel*.

## Chapter 10

# IEC Coupler impedances

The Comsol model with which this data is gathered exports the input impedance correctly, but the transfer impedance is actually the *negative* of the actual transfer impedance. This is due to Comsol, which was only interested in the magnitude of the impedance values, and due to us (sloppy work). The input impedance is defined as:

$$Z_{\text{in}} = \frac{P_{\text{coupler,entrance}}}{U_{\text{coupler,entrance}}} \quad (10.1)$$

and the transfer impedance as:

$$Z_{\text{tr}} = \frac{P_{\text{DRP}}}{U_{\text{coupler,entrance}}} \quad (10.2)$$

## Chapter 11

# Kampinga's SLNS model in our notation

### 11.1 Model

$$\nabla^2 h_v + \frac{2}{i\delta_v^2} h_v = 0, \quad (11.1)$$

$$\nabla^2 h_\kappa + \frac{2}{i\delta_\kappa^2} h_\kappa = 0, \quad (11.2)$$

$$\frac{1}{k} \nabla \cdot ((1 - h_v) \nabla p) + k (1 + (\gamma - 1) h_\kappa) p = 0 \quad (11.3)$$

The velocity is:

$$\mathbf{u} = \frac{i}{\rho_0 \omega} (1 - h_v) \nabla p \quad (11.4)$$

With boundary conditions:

$$h_v = 1 \quad \text{at the wall} \quad (11.5)$$

$$h_\kappa = 1 \quad \text{at the wall} \quad (11.6)$$

For pressure / velocity b.c.'s

$$\mathbf{u} = \frac{i}{\rho_0 \omega} (1 - h_v) \nabla p \quad (11.7)$$

Weak contribution in pressure acoustics interface:

$$(\text{hnu} * (\text{test}(px) * px + \text{test}(py) * py + \text{test}(pz) * \text{test}(pz)) + \text{test}(p) * p * \text{acpr} . ik^2 * (1 - \text{gamma}) * \text{hkappa}) \quad (11.8)$$

# Bibliography

- [1] R.B. Bird, W.E. Stewart, and E.N. Lightfoot. *Transport phenomena*. 2nd. Wiley International edition. New York, NY, USA: J. Wiley, 2007. ISBN: 978-0-470-11539-8.
- [2] D.T. Blackstock. *Fundamentals of physical acoustics*. Hoboken, NJ, USA: John Wiley & Sons, 2000. 541 pp.
- [3] J.A. De Jong. “Numerical modeling of thermoacoustic systems.” PhD thesis. Enschede: Universiteit Twente, 2015. URL: <http://doc.utwente.nl/96275/>.
- [4] F.J.M. van der Eerden. “Noise reduction with coupled prismatic tubes.” PhD thesis. Enschede, The Netherlands: University of Twente, Nov. 2000.
- [5] W.R. Kampinga. “Viscothermal acoustics using finite elements: analysis tools for engineers.” PhD thesis. Enschede, The Netherlands: University of Twente, 2010.
- [6] FC Karal. “The analogous acoustical impedance for discontinuities and constrictions of circular cross section.” In: *The Journal of the Acoustical Society of America* 25.2 (1953), pp. 327–334.
- [7] Naoki Kino et al. “Investigation of non-acoustical parameters of compressed melamine foam materials.” In: *Applied Acoustics* 70.4 (Apr. 2009), pp. 595–604. ISSN: 0003682X. DOI: [10.1016/j.apacoust.2008.07.002](https://doi.org/10.1016/j.apacoust.2008.07.002). URL: <https://linkinghub.elsevier.com/retrieve/pii/S0003682X08001497> (visited on 11/28/2019).
- [8] William Licht and Dietrich G. Stechert. “The Variation of the Viscosity of Gases and Vapors with Temperature.” In: *The Journal of Physical Chemistry* 48.1 (1944), pp. 23–47. ISSN: 0092-7325. DOI: [10.1021/j150433a004](https://doi.org/10.1021/j150433a004). (Visited on 01/08/2015).
- [9] M. J. J. Nijhof. “Viscothermal wave propagation.” PhD thesis. E: University of Twente, 2010.
- [10] Sjoerd W Rienstra and Avraham Hirschberg. “An introduction to acoustics.” In: *Eindhoven University of Technology* 18 (2015), p. 296.
- [11] Nikolaus Rott. “Damped and thermally driven acoustic oscillations in wide and narrow tubes.” In: *Zeitschrift für angewandte Mathematik und Physik* 20.2 (Mar. 1969), pp. 230–243. ISSN: 0044-2275. DOI: [10.1007/BF01595562](https://doi.org/10.1007/BF01595562).
- [12] G. W. Swift. “Thermoacoustic Engines.” In: *The Journal of the Acoustical Society of America* 84.4 (1988), pp. 1145–1180. ISSN: 00014966. DOI: [10.1121/1.396617](https://doi.org/10.1121/1.396617). (Visited on 07/20/2011).
- [13] G. W. Swift. *Thermoacoustics: A unifying perspective for some engines and refrigerators*. Melville, NY, USA: Acoustical Society of America, 2003. 315 pp.
- [14] H. Tijdeman. “On the propagation of sound waves in cylindrical tubes.” In: *Journal of Sound and Vibration* 39.1 (Mar. 8, 1975), pp. 1–33. ISSN: 0022-460X. DOI: [10.1016/S0022-460X\(75\)80206-9](https://doi.org/10.1016/S0022-460X(75)80206-9). (Visited on 01/05/2012).
- [15] W. C. Ward, J. P. Clark, and G. W. Swift. *DeltaEC Users Guide version 6.4b2.7*. Dec. 4, 2017. URL: [www.lanl.gov/thermoacoustics](http://www.lanl.gov/thermoacoustics) (visited on 01/22/2018).

## Appendix A

# Thermal relaxation in thick tubes

### A.1 Thermal relaxation effect in thick tubes

In this section, a formulation for  $\epsilon_s$  is given for tubes where the temperature wave in the solid is present. Figure A.1 shows a schematic overview of the situation. As shown in the figure, the temperature wave accompanied with an acoustic wave results in heat conduction to/from the wall of the tube. To solve this interaction mathematically, the heat equation in the solid has to be solved. For constant thermal conductivity, density and heat capacity the heat equation of the solid is

$$\rho_s c_s \frac{\partial \tilde{T}_s}{\partial t} = \kappa_s \nabla^2 \tilde{T}_s, \quad (\text{A.1})$$

where  $\rho_s$ ,  $c_s$ ,  $\tilde{T}_s$  and  $\kappa_s$  are the density, specific heat, temperature and thermal conductivity of the solid, respectively. In frequency domain and using cylindrical coordinates, assuming axial symmetry, this can be written as

$$\left( r^2 \left( \frac{\partial^2}{\partial r^2} + \frac{\partial^2}{\partial x^2} \right) + r \frac{\partial}{\partial r} + \frac{2}{i\delta_s^2} r^2 \right) T_s = 0, \quad (\text{A.2})$$

where  $\delta_s$  is

$$\delta_s = \sqrt{\frac{2\kappa_s}{\rho_s c_s \omega}}. \quad (\text{A.3})$$

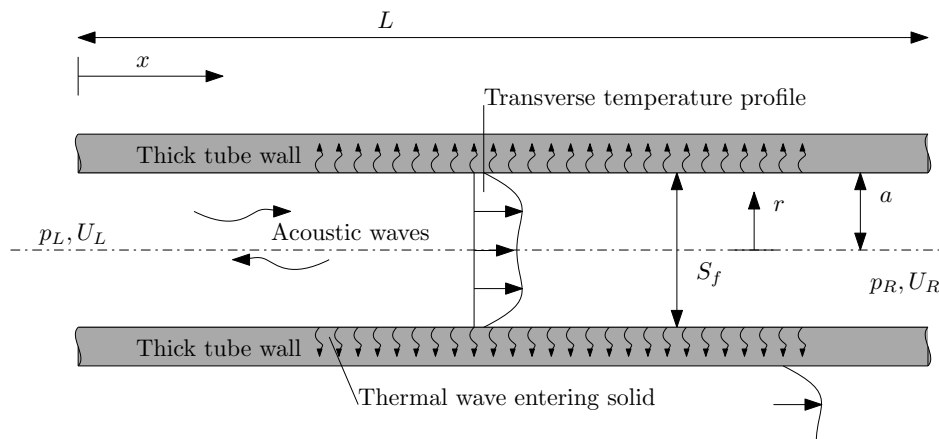


**Figure A.1** – Schematic situation of a tube surrounded by a thick solid. Note that the transverse acoustic temperature is drawn to be not zero at the wall. This happens in case of thermal interaction with a solid with finite thermal effusivity.

Now, since  $\partial T_s / \partial x \sim \frac{\delta_s}{\lambda} \frac{\partial T_s}{\partial r}$ , the second order derivative of the temperature in the axial direction can be neglected. In that case, the differential equation to solve for is

$$\left( r^2 \frac{\partial^2}{\partial r^2} + r \frac{\partial}{\partial r} + \frac{2}{i\delta_s^2} r^2 \right) T_s = 0, \quad (\text{A.4})$$

which is a Bessel differential equation of the zero'th order in  $T_s$ . The solutions is sought in terms of traveling cylindrical waves:

$$T_s = C_1 H_0^{(1)} \left( (i-1) \frac{r}{\delta_s} \right) + C_2 H_0^{(2)} \left( (i-1) \frac{r}{\delta_s} \right), \quad (\text{A.5})$$

where  $C_1$  and  $C_2$  constants to be determined from the boundary conditions, and  $H_\alpha^{(i)}$  is the cylindrical Hankel function of the  $(i)^{\text{th}}$  kind and order  $\alpha$ . If we require  $T_s \rightarrow 0$  as  $r \rightarrow \infty$ , the constant  $C_2$  is required to be 0. From the acoustic energy equation, a similar differential equation can be found for the acoustic temperature in the fluid:

$$\left( r^2 \frac{\partial^2}{\partial r^2} + r \frac{\partial}{\partial r} + \frac{2}{i\delta_s^2} r^2 \right) T = \frac{2}{i\delta_s^2} \frac{\alpha_p T_0}{\rho_0 c_p} p,$$

for which the (partial) solution is

$$T = \frac{\alpha_p T_0}{\rho_0 c_p} p \left( 1 - C_3 J_0 \left( (i-1) \frac{r}{\delta_\kappa} \right) \right). \quad (\text{A.6})$$

To attain at Eq. A.6, use has been made of the fact that the temperature should be finite at  $r = 0$ .  $C_3$  is a constant that is to be determined from the boundary conditions at the solid-fluid interface. These boundary conditions are:

$$T_s|_{r=a} = T|_{r=a}, \quad (\text{A.7})$$

$$-\kappa_s \frac{\partial T_s}{\partial r}|_{r=a} = -\kappa \frac{\partial T}{\partial r}|_{r=a}, \quad (\text{A.8})$$

i.e. continuity of the temperature and the heat flux at the interface. This yields two equations for two unknowns ( $C_1$  and  $C_3$ ,  $C_2$  is already argued to be 0). Solving for the acoustic temperature yields:

$$T = \frac{\alpha_p T_0}{\rho_0 c_p} p \left( 1 - \frac{1}{(1 + \epsilon_s)} \frac{J_0 \left( (i-1) \frac{r}{\delta_\kappa} \right)}{J_0 \left( (i-1) \frac{a}{\delta_\kappa} \right)} \right) p,$$

where

$$\epsilon_s = \frac{e_f J_1 \left( (i-1) \frac{a}{\delta_\kappa} \right) H_0^{(1)} \left( (i-1) \frac{a}{\delta_s} \right)}{e_s J_0 \left( (i-1) \frac{a}{\delta_\kappa} \right) H_1^{(1)} \left( (i-1) \frac{a}{\delta_s} \right)}, \quad (\text{A.9})$$

where  $e_f$  is the thermal effusivity of the fluid, and  $e_s$  the thermal effusivity of the solid, such that the ratio is

$$\frac{e_f}{e_s} = \sqrt{\frac{\kappa \rho_0 c_p}{\kappa_s \rho_s c_s}}. \quad (\text{A.10})$$

Note that for large  $a/\delta_\kappa$ :

$$\frac{J_1 \left( (i-1) \frac{a}{\delta_\kappa} \right)}{J_0 \left( (i-1) \frac{a}{\delta_\kappa} \right)} \rightarrow i, \quad (\text{A.11})$$

and for large  $a/\delta_s$

$$\frac{H_0^{(1)} \left( (i-1) \frac{a}{\delta_s} \right)}{H_1^{(1)} \left( (i-1) \frac{a}{\delta_s} \right)} \rightarrow -i, \quad (\text{A.12})$$

such that for both numbers large

$$\epsilon_s \rightarrow \frac{e_f}{e_s}. \quad (\text{A.13})$$

## Appendix B

# Derivation of Karal's discontinuity factor

**Note: this documentation is incomplete.**

This appendix describes the derivation of Karal's discontinuity factor. The following assumptions underlie the model:

- $z = 0$  : position of the discontinuity
- Assume  $f \ll f_c$ , such that far away from the discontinuity, only propagating modes exist.
- Assume axial symmetry, so dependence of  $\theta$  is dropped

In cylindrical coordinates, the solution of the Helmholtz equation can be written in terms of cylindrical harmonics [2]. Assuming axial symmetry such that the acoustic pressure in for example tube  $B$  can be written as:

$$p_B = \begin{Bmatrix} J_m(k_r r) \\ N_m(k_r r) \end{Bmatrix} \begin{Bmatrix} e^{im\phi} \\ e^{-im\phi} \end{Bmatrix} \begin{Bmatrix} e^{\beta z} \\ e^{-\beta z} \end{Bmatrix} \quad (\text{B.1})$$

where  $J_m$  is the cylindrical Bessel function of order

$$k_r^2 - \beta^2 = k^2. \quad (\text{B.2})$$

Using the boundary condition that

$$\frac{\partial p_B}{\partial r} \Big|_{r=b} = 0, \quad (\text{B.3})$$

and assuming axial symmetry (only the  $m = 0$  modes) it follows that

$$\frac{\partial J_0}{\partial r}(k_r b) \Big|_{r=b} = 0. \quad (\text{B.4})$$

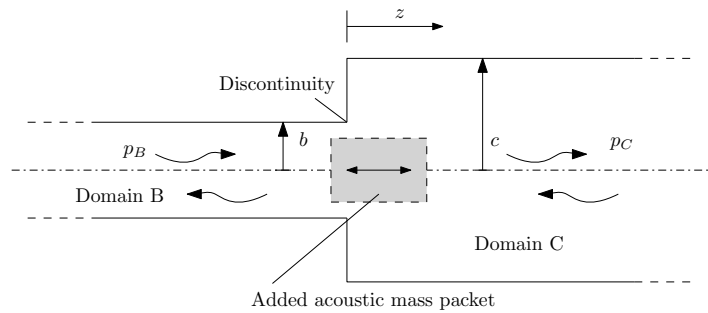


**Figure B.1** – Schematic of a discontinuity at the interface between two tubes with different radius. Domain B is the smaller tube and domain C is the larger tube. The radius of the tube in domain B is  $b$ , and the radius of the tube in domain C is  $c$ .

Assuming that  $\alpha_k$  is the  $k^{\text{th}}$  zero of  $J'_0(x)$ , we can write for  $k_{r,k}$ :

$$k_{r,k} = \frac{\alpha_k}{b}. \quad (\text{B.5})$$

Hence we find the following reduced expression for the pressure in tube  $B$ :

$$p_B = B_0^0 \exp(ikz) + B_0^1 \exp(-ikz) + \sum_{n=1}^{\infty} B_n J_0\left(\alpha_n \frac{r}{b}\right) \left\{ \begin{array}{l} e^{\beta_n z} \\ e^{-\beta_n z} \end{array} \right\}, \quad (\text{B.6})$$

where accordingly,

$$\beta_k^2 = \left(\frac{\alpha_k}{b}\right)^2 - k^2 \quad (\text{B.7})$$

For  $k^2 < (\alpha_k/b)^2$ ,  $\beta_k^2 > 0$ , the modes are evanescent. And since we only allow finite solutions for  $z \leq 0$ , the final results for  $p_B$  is

$$p_B = B_0^0 \exp(ikz) + B_0^1 \exp(-ikz) + \sum_{n=1}^{\infty} B_n J_0\left(\alpha_n \frac{r}{b}\right) e^{\beta_n z}, \quad (\text{B.8})$$

where  $\beta_n$  is defined as the positive root of the r.h.s. of Eq. B.7. We simplify this relation to:

$$p_B(z) = p_B^0(z) + \sum_{n=1}^{\infty} B_n J_0\left(\alpha_n \frac{r}{b}\right) e^{\beta_n z}. \quad (\text{B.9})$$

For the velocity we find

$$u_B(z) = u_B^0(z) + \sum_{n=1}^{\infty} Y_{B,n} B_n J_0\left(\alpha_n \frac{r}{b}\right) e^{\beta_n z}, \quad (\text{B.10})$$

where

$$Y_{B,n} = \frac{i\beta_n}{\omega\rho_0}. \quad (\text{B.11})$$

Similarly, for the positive  $z$  we find

$$p_C(z) = p_C^0(z) + \sum_{m=1}^{\infty} C_m J_0\left(\alpha_m \frac{r}{c}\right) e^{-\gamma_m z}, \quad (\text{B.12})$$

where

$$\gamma_m = \sqrt{\left(\frac{\alpha_m}{c}\right)^2 - k^2}. \quad (\text{B.13})$$

and

$$u_C(z) = u_C^0(z) + \sum_{m=1}^{\infty} Y_{C,m} C_m J_0\left(\alpha_m \frac{r}{c}\right) e^{-\gamma_m z}, \quad (\text{B.14})$$

where

$$Y_{C,m} = -\frac{i\gamma_m}{\omega\rho_0} \quad (\text{B.15})$$

## B.1 Boundary conditions

At the interface ( $z = 0$ ), the following boundary conditions are valid:

$$u_B|_{z=0} = u_C|_{z=0} \quad 0 \leq r \leq b \quad (\text{B.16})$$

$$u_C|_{z=0} = 0 \quad b \leq r \leq c \quad (\text{B.17})$$

$$p_B = p_C \quad 0 \leq r \leq b \quad (\text{B.18})$$

Taking Eq. B.16, multiply by  $r$  and integrating from 0 to  $c$ , taking into account Eq. B.17 yields:

$$b^2 u_B^0 = c^2 u_C^0 \quad (\text{B.19})$$

We require one more equation at the interface, which is found from the continuity boundary conditions as well. Multiplying Eq. B.16 with  $J_0(\alpha_q \frac{r}{c})r$  and integrating setting  $q = m$  and dividing by  $bc$  yields:

$$u_B^0 J_1(\alpha_m \rho) \frac{1}{\alpha_q} + \sum_{n=1}^{\infty} Y_{B,n} T_{mn} B_n = Y_{C,m} \frac{1}{2} \rho^{-1} J_0(\alpha_m)^2 C_m, \quad (\text{B.20})$$

where

$$T_{mn} = \frac{\alpha_m}{\alpha_m^2 - \frac{\alpha_n^2}{\rho^2}} J_0(\alpha_n) J_1(\alpha_m \rho). \quad (\text{B.21})$$

Setting  $p_B = p_C$

$$p_B^0 = p_C^0 + 2 \sum_{m=1}^{\infty} \frac{J_1(\alpha_m \rho)}{\rho \alpha_m} C_m \quad (\text{B.22})$$

$$B_n J_0(\alpha_n)^2 = \frac{2}{\rho} \sum_{m=1}^{\infty} T_{mn} C_m \quad (\text{B.23})$$

$$\sum_{n=1}^{\infty} \frac{2\alpha_n}{J_0(\alpha_n)^2} T_{mn} \sum_{q=1}^{\infty} T_{qn} D_q + \frac{1}{2} \rho \alpha_m J_0(\alpha_m)^2 D_m = J_1(\alpha_m \rho) \frac{\rho}{\alpha_m}, \quad (\text{B.24})$$

where

$$D_m = \frac{C_m}{ikb u_B^0 z_0} \quad (\text{B.25})$$

Eq. B.24 is a set of infinite equations in terms of an infinite number of unknowns for  $D_m$ . In matrix algebra for a finite set, this can be written as

$$(\mathbf{M}_1 \cdot \mathbf{M}_2 + \mathbf{K}) \cdot \mathbf{D} = \mathbf{R} \quad (\text{B.26})$$

where

$$M_{1,ij} = \frac{2\alpha_j}{J_0(\alpha_j)^2} T_{ij} \quad (\text{B.27})$$

$$M_{2,ij} = T_{ji} \quad (\text{B.28})$$

$$K_{ij} = \frac{1}{2} \rho \alpha_j J_0(\alpha_j)^2 \quad ; \quad i = j \quad (\text{B.29})$$

$$K_{ij} = 0 \quad ; \quad i \neq j \quad (\text{B.30})$$

$$R_i = J_1(\alpha_i \rho) \frac{\rho}{\alpha_i} \quad (\text{B.31})$$

Finally, the added acoustic mass,

$$p_C^0 = p_B^0 - i\omega M_A U_B, \quad (\text{B.32})$$

can be computed as

$$\rho_0 \sum_{m=1}^{\infty} \frac{2}{\pi b} \frac{J_1(\alpha_m \rho)}{\rho \alpha_m} D_m \quad (\text{B.33})$$

For a given velocity  $u_{C,0}$  the velocity profile at  $z = 0$  is

$$u_C = u_C^0 + b u_B^0 \sum_{m=1}^{\infty} \gamma_m D_m J_0\left(\alpha_m \frac{r}{c}\right) \quad (\text{B.34})$$